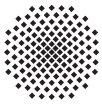

Universität Stuttgart

SimTech
Cluster of Excellence

R. Helmig · J. Niessner · B. Flemisch · M. Wolff · J. Fritz

Efficient modelling of flow and transport in porous media using multi-physics and multi-scale approaches

Stuttgart, April 2010

Institute of Hydraulic Engineering,
Dept. of Hydromechanics and Modeling of Hydrosystems,
University of Stuttgart,
Pfaffenwaldring 61, 70569 Stuttgart/ Germany
{rainer.helmig,jennifer.niessner,bernd.flemisch,markus.wolff,jochen.fritz}@iws.uni-stuttgart.de
www.hydrosys.uni-stuttgart.de

Abstract. Flow and transport processes in porous media including multiple fluid phases are the governing processes in a large variety of geological and technical systems. In general, these systems include processes of different complexity occurring in different parts of the domain of interest. The different processes mostly also take place on different spatial and temporal scales. It is extremely challenging to model such systems in an adequate way accounting for the spatially varying and scale-dependent character of these processes. In this work, we give a brief overview of existing upscaling, multi-scale, and multi-physics methods, and we present mathematical models and model formulations for multi-phase flow in porous media including compositional and non-isothermal flow. Finally, we show simulation results for two-phase flow using a multi-physics method and a multi-scale multi-physics algorithm.

Contents

1 Introduction 2
2 State of the art 4
3 Mathematical models for flow and transport processes in porous media 8
4 Numerical solution approaches 19
5 Application of multi-physics and multi-scale methods 22
6 Conclusion 28

Preprint Series **Issue No. 2010-27**
Stuttgart Research Centre for Simulation Technology (SRC SimTech)
SimTech – Cluster of Excellence
Pfaffenwaldring 7a
70569 Stuttgart
publications@simtech.uni-stuttgart.de
www.simtech.uni-stuttgart.de

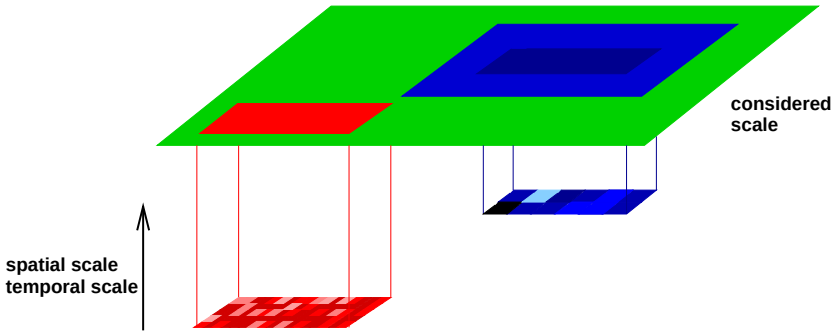

Fig. 1 A general physical system where different processes occur in different parts of a domain and on different scales.

1 Introduction

Within hydrological, technical or biological systems, various processes generally occur within different sub-domains. These processes must be considered on different space and time scales, and they require different model concepts and data. Highly complex processes may take place in one part of the system necessitating a fine spatial and temporal resolution, while in other parts of the system, physically simpler processes take place allowing an examination on coarser scales. Considering the porous medium, its heterogeneous structure shows a high dependence on the spatial scale ([101]).

Figure 1 shows a general physical system which typically consists of certain subregions. The darker regions represent subdomains of the total system dominated by other physical processes than the light part. These processes take place on finer spatial and temporal scales. While traditional models describe this system on one scale – this must be the fine scale if an accurate description is desired – **multi-scale** algorithms take the dependence of the processes on both spatial and temporal scales into account, where the connection between both scales is made by up- and downscaling approaches. Much research has been done to upscale either pressure or saturation equation in two-phase flow or include the different scales directly in the numerical scheme by using multi-scale finite volumes or elements, see e.g. [30, 33, 46, 48, 49, 51, 52, 72, 81, 112].

In constrast to the abilities of traditional models, **multi-physics** approaches allow to apply different model concepts in different subdomains. Like that, in the black part of the domain, other processes can be accounted for than in the lighter subdomains. In this respect, research has advanced in the context of domain decomposition techniques (see e.g. [134, 138]) and in the context of mortar finite element techniques that allow multi-physics as well as multi-numerics coupling (see e.g. [109]).

The advantage of multi-scale multi-physics algorithms is that they require much less data as if using the fine-scale model in the whole domain. Additionally, they allow to save computing time or make the computation of very complex and large systems possible that could otherwise not be numerically simulated.

In the following, as an example application, the storage of carbon dioxide (CO_2) in a deep geological formation will be studied and multi-scale as well as multi-physics aspects in space and time will be identified. Please note that multi-scale and multi-physics aspects are relevant in a large number of additional applications, not only in geological systems, but also in biological (e.g. treatment of brain tumors) and technical (e.g. processes in polymer electrolyte membrane fuel cells) systems. Thus, multi-scale multi-physics techniques developed for geological applications can be transferred to a broad range of other problems.

Concerning CO_2 storage, different storage options are commonly considered that are shown in Figure 2, which is taken from [78]. According to that figure, possible storage possiblities are given by depleted oil and gas reservoirs, use of CO_2 in the petroleum industry in order to enhance oil and gas recovery or – in a similar spirit – in order to improve the methane production by injection of CO_2. Besides, deep saline formations represent possible storage places, either onshore or offshore. When injecting carbon dioxide, processes take place on highly different spatial and temporal scales. Concerning spatial scales, the processes in the vicinity of the CO_2 plume are very complex including phase change, chemical reactions etc. But usually, the interest lies on the effect of the CO_2 injection on larger domains, especially if it is to be investigated whether CO_2 is able to migrate to the surface or

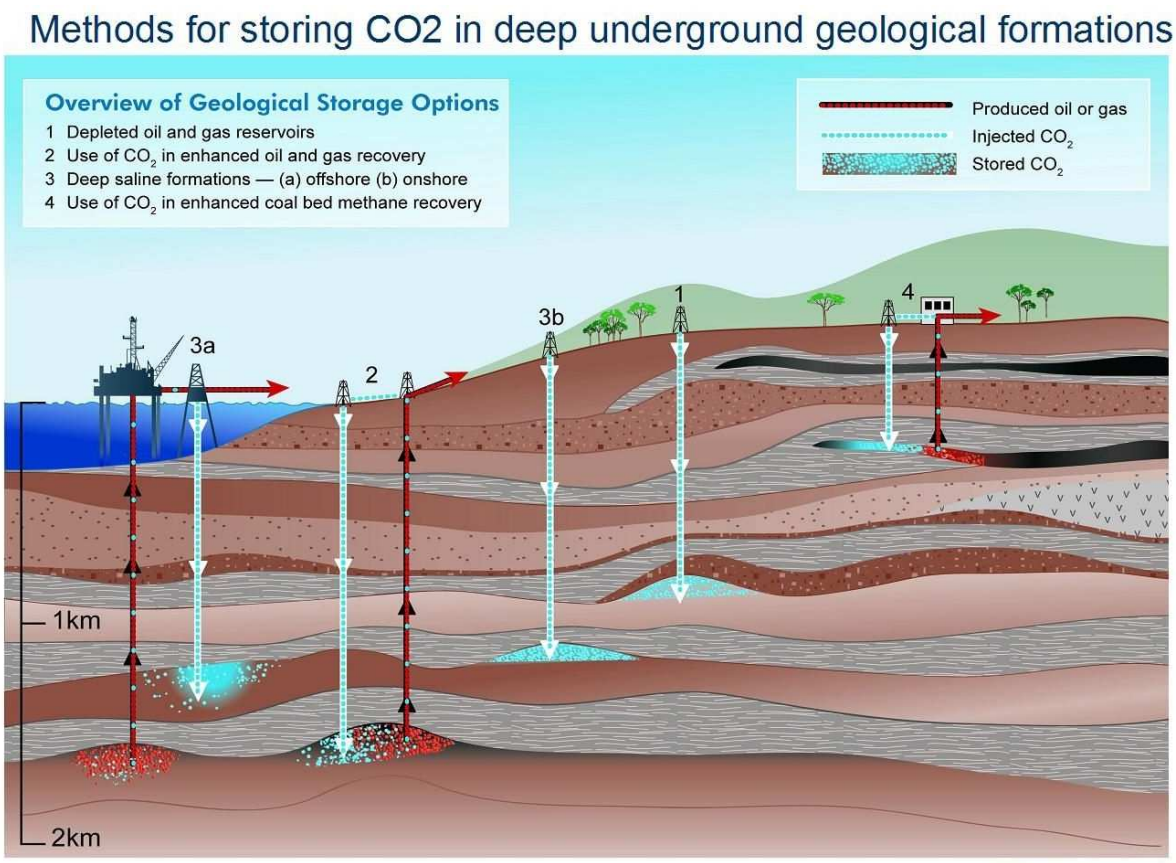

Fig. 2 Carbon dioxide storage scenarios from IPCC special report on carbon capture and storage, [78].

not. In the vicinity of the CO_2 plume, processes of much higher complexity and much higher fine-scale dependence occur than in the remaining part of the domain. This aspect prescribes both the spatial multi-scale and the spatial multi-physics character of this application: around the CO_2 plume, processes have to be resolved on a fine spatial scale in order to be appropriately accounted for. In the rest of the domain of interest, processes may be resolved on a coarser spatial scale. Additionally, the processes occurring in the plume zone and in the non-plume zone are different: While highly complex three-phase three-component processes including reaction need to be considered near the plume, further away from the plume, the consideration of a single-phase system may be sufficient.

With respect to spatial scales we consider Figure 3, which is again taken from [78]. In the early time period, i.e. few years after the CO_2 injection ceased, the movement of the CO_2 is determined by advection-dominated multi-phase flow (viscous, buoyant, and capillary effects are relevant). In a later time period, when the CO_2 has reached residual saturation everywhere, dissolution and diffusion processes are most decisive for the migration of the carbon dioxide. Eventually, in the very long time range of thousands of years, it is to be expected that the CO_2 will be bound by chemical reactions.

This paper is structured as follows: In Section 2, we define the relevant scales considered in this work and give an overview of multi-scale and of multi-physics techniques. Next, in Section 3, the mathematical model for flow and transport in porous media is described including non-isothermal flow and different mathematical formulations. In Section 4, the numerical solution procedures for both decoupled and coupled model formulations are explained. In Section 5, we present two different applications of multi-physics and of multi-scale multi-physics algorithms. Finally, we conclude in Section 6.

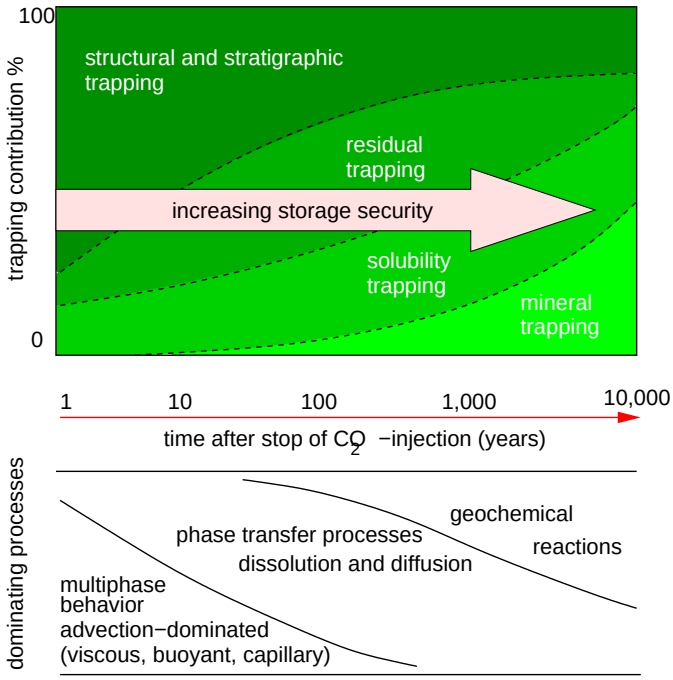

Fig. 3 Time scales of carbon dioxide sequestration, [78].

2 State of the art

We want to give a brief introduction into existing multi-scale methods and into methods for scale transfer. First, general definitions of different important scales are given (Section 2.1) to point out which are the scales considered in the following sections. Afterwards, we give a very general overview of basic approaches for upscaling (Section 2.2) and different kinds of multi-scale methods (Sec. 2.2.2), and a short introduction to multi-physics methods (Sec. 2.3).

2.1 Definition of scales

In order to design an appropriate modeling strategy for particular problems, it is important to consider the spatial and temporal scales involved, and how the physical processes and parameters of the system relate to these scales.

A careful definition of relevant length scales can clarify any investigation of scale considerations, although such definitions are a matter of choice and modeling approach [73]. In general, we define the following length scales of concern: the molecular length scale, which is of the order of the size of a molecule; the microscale, or the minimum continuum length scale on which individual molecular interactions can be neglected in favor of an ensemble average of molecular collisions; the local scale, which is the minimum continuum length scale at which the microscale description of fluid movement through individual pores can be neglected in favor of averaging the fluid movement over a representative elementary volume (REV) – therefore this scale is also called the REV-scale; the mesoscale, which is a scale on which local scale properties vary distinctly and markedly; and the megascale or field-scale. Measurements or observations can yield representative information across this entire range of scales, depending on the aspect of the system observed and the nature of the instrument used to make the observation. For this reason, we do not specifically define a measurement scale.

Figure 4 graphically depicts the range of spatial scales of concern in a typical porous medium system. It illustrates two important aspects of these natural systems: several orders of magnitude in potentially relevant length scales exist, and heterogeneity occurs across the entire range of relevant scales. A similar range of temporal scales exists as well, from the pico-seconds over which a chemical

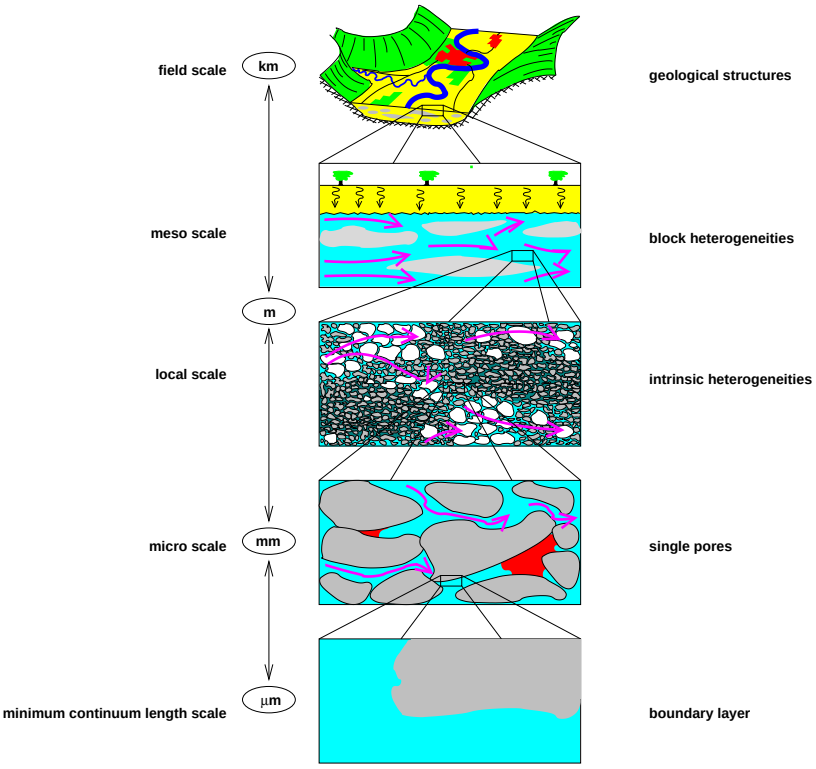

Fig. 4 Different scales for flow in porous media

reaction can occur on a molecular length scale to the centuries or milleniums of concern in the long-term storage of greenhouse gases or atomic waste.

When looking at the REV-scale, we average over both fluid–phase properties and solid–phase properties. In Figure 5, we schematically show the averaging behavior on the example of the porosity. While averaging over a representative elementary volume (REV), we assume that the averaged property P does not oscillate significantly. In Figure 5 this is the case in the range of r_{min} to r_{max}, so an arbitrarily shaped volume V with an inscribed sphere with radius r_{min} and a circumscribed sphere with radius r_{max} can be chosen as REV. Accordingly, we do not assume any heterogeneities on the REV-scale. For our model, we assume that the effects of the sub–REV–scale heterogeneities are taken into account by effective parameters.

The scales of interest in this work are the meso-scale (which we also call fine scale) and the mega-scale (for us, the coarse scale).

2.2 Upscaling and multi-scale methods

In multi-scale modeling, more than one scale is involved in the modeling as the name implies. In general, each pair of scales is coupled in a bidirectional way, where the coarser scale contains the finer scale. This means that upscaling and downscaling methods have to be provided. Upscaling is a transition of the finer to the coarser scale and downscaling vice-versa. Both kinds of operators are generally needed. Only special applications with weak coupling between the scales allow for a mono-directional coupling and thus, only upscaling or only downscaling operators.

Classical upscaling strategies comprise the method of asymptotic expansions (homogenization) and volume averaging. Usually, the fine-scale informations which get lost due to averaging are acconted for by effective parameters in the upscaled equations. For downscaling, the typical methodology is to specify boundary conditions at the boundaries of a coarse-grid block and solve a fine-grid problem in the respective domain. The boundary conditions are obtained either directly from the coarse-scale problem or coarse-scale results are rescaled to fine-scale properties using fine-scale material parameters. In the

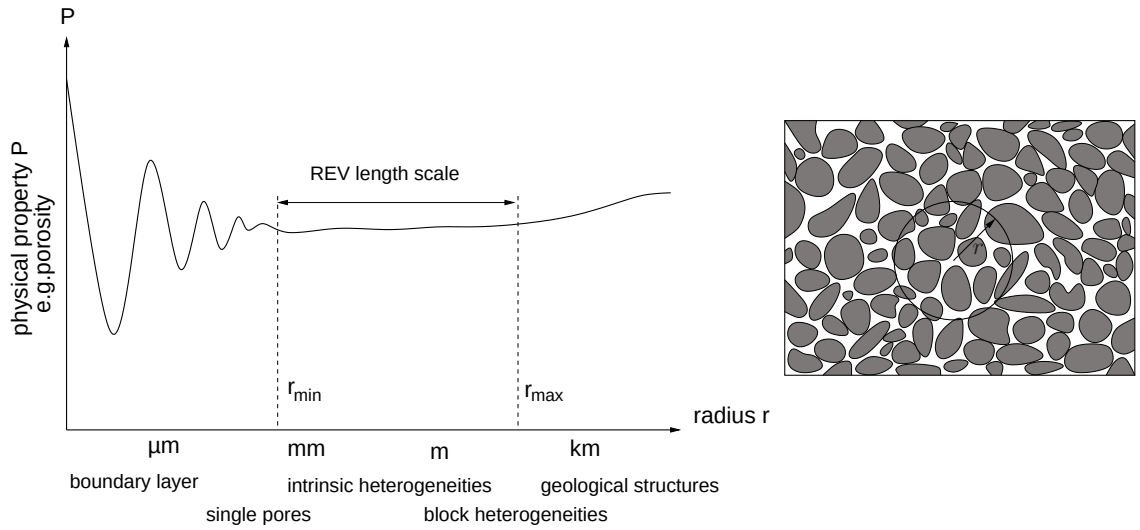

Fig. 5 Different scales for flow in porous media (schematically for Figure 4)

latter case, fine-grid boundary conditions can be specified along the boundaries of the downscaling domain.

In the following, we provide a brief overview of common upscaling techniques and of multi-scale methods.

2.2.1 Upscaling methods

Effective Coefficients This method the coarse scale equations to be a priori known, for example by assuming the same kind of equation than at the fine scale. In that case the problem is to find upscaled or averaged effective model parameters to describe the physical large scale behavior properly. This method is very commonly applied to upscale the single-phase flow equation in porous media. Effective parameters like the transmissibility are obtained by the solution of local fine-scale problems which can be isolated from the global problem (local upscaling) or coupled to the global problem (local-global upscaling) (e.g., see [46] or [30]).

Pseudo Functions This method follows the idea of effective coefficients described before. The question is how to determine effective parameters like coarse-scale relative permeabilities, mobilities or fractional flow functions, which depend on the primary variables and therefore vary in time. One possibility, which is for example discussed in [14] and [40], is the use of pseudo functions. Most likely, these functions are calculated from the solution of a fine-scale multi-phase flow problem (e.g., see [29]). Detailed investigations on appropriate boundary conditions for the solution of the local fine scale problems can be found in [130] and [131].

Volume Averaging/Homogenization Methods These methods allow to derive new coarse scale equations from known fine-scale equations. Volume averaging methods applied on porous media flow can for example be found in [135] or [64], homogenization methods are applied in [106]. A problem of this averaging approaches is the determination of new constitutive relations appearing in the upscaled coarse-scale equations, which describe the influence of fine scale fluctuations on the averaged coarse scale solution. For two-phase flow approaches to calculate terms including fine-scale fluctuations into the coarse-scale equations are developed for example by [52] and [51].

2.2.2 Multi-scale methods

Homogeneous multi-scale methods Homogeneous multi-scale methods inherently give approximate solutions on the micro-scale. They consist of the traditional numerical approaches to deal with multi-scale problems, like, e.g., multi-grid methods, [20, 24, 123, 127], multi-resolution wavelet methods,

[26, 67, 80, 128], multi-pole techniques, [62, 104, 125, 137], or adaptive mesh refinement, [5, 13, 98]. Due to the usually enormous number of degrees of freedom on this scale, this direct numerical solution of real-world multiple scale problems is impossible to realize even with modern supercomputers.

Heterogeneous multi-scale methods The heterogeneous multi-scale method (HMM), [50], proposes general principles for developing accurate numerical schemes for multiple problems, while keeping costs down. It was first introduced in [47], and clearly described in [48]. The general goal of the HMM, as in other multi-scale type methods, is to capture the macroscopic behavior of multi-scale solutions without resolving all the fine details of the problem. The HMM does this by selectively incorporating the microscale data when needed, and exploiting the characteristics of each particular problem.

Variational multi-scale method In [75, 76], the authors present the variational multi-scale method that serves as a general framework for constructing multi-scale methods. An important part of the method is to split the function space into a coarse part, which captures low frequencies, and a fine part, which captures the high frequencies. An approximation of the fine-scale solution is computed and it is used to modify the coarse-scale equations. In recent years, there have been several works on convection-diffusion problems using the variational multi-scale framework, see, e.g. [39, 66, 83].

Multi-scale finite volume method The underlying idea is to construct transmissibilities that capture the local properties of the differential operator. This leads to a multi-point discretization scheme for the finite volume solution algorithm. The transmissibilities can be computed locally and therefore this step is perfectly suited for massively parallel computers. Furthermore, a conservative fine-scale velocity field can be constructed from the coarse-scale pressure solution. Over the recent years, the method became able to deal with increasingly complex equations, [65, 82, 89, 92–94].

Multi-scale finite element method Another multi-scale method, the multi-scale finite element method, was presented in 1997, [72]. The theoretical foundation is based on homogenization theory. The main idea is to solve local fine-scale problems numerically in order to use these local solutions to modify the coarse-scale basis functions. There has been a lot of work on this method over the last decade, see, e.g. [1, 2, 9, 53, 85, 86].

Multi-scale methods and domain decomposition By comparing the formulations, the authors of [103] observe that the multi-scale finite volume method is a special case of a nonoverlapping domain decomposition preconditioner. They go on to suggest how the more general framework of domain decomposition methods can be applied in the multi-scale context to obtain improved multi-scale estimates.

2.3 Multi-physics methods

In general, the term multi-physics is used whenever processes which are described by different sets of equations interact and thus are coupled within one global model. The coupling mechanisms can in general be divided into volume (or vertical) coupling and surface (or horizontal) coupling. In this sense, the multi-scale approaches introduced before could be interpreted as vertical coupling approaches. Moreover, a large variety of multi-continua models exist. Here, the model domain is physically the same for the different sets of equations, and the exchange is usually performed by means of source and sink terms. Within the context of porous media, most well-known multi-continua models include the double porosity models, [8, 114], and the MINC method (Multiple INteracting Continua), [111, 119].

In contrast to that, horizontal coupling approaches divide the model domain into subdomains sharing common interfaces. The coupling is achieved by enforcing appropriate interface conditions. In physical terms, these interface conditions should state thermodynamic equilibrium (mechanical, thermal, and chemical equilibrium), while in mathematical terms, they often correspond to the continuity of the employed primal and dual variables, like, e.g., pressure and normal velocity. Examples for surface coupling are discrete fracture approaches, [43], or the coupling of porous media flow and free flow domains, [17, 44, 63, 79, 88]. While these two examples couple two different flow regimes, we will in our study concentrate on the coupling of different processes inside one porous media domain. In [6],

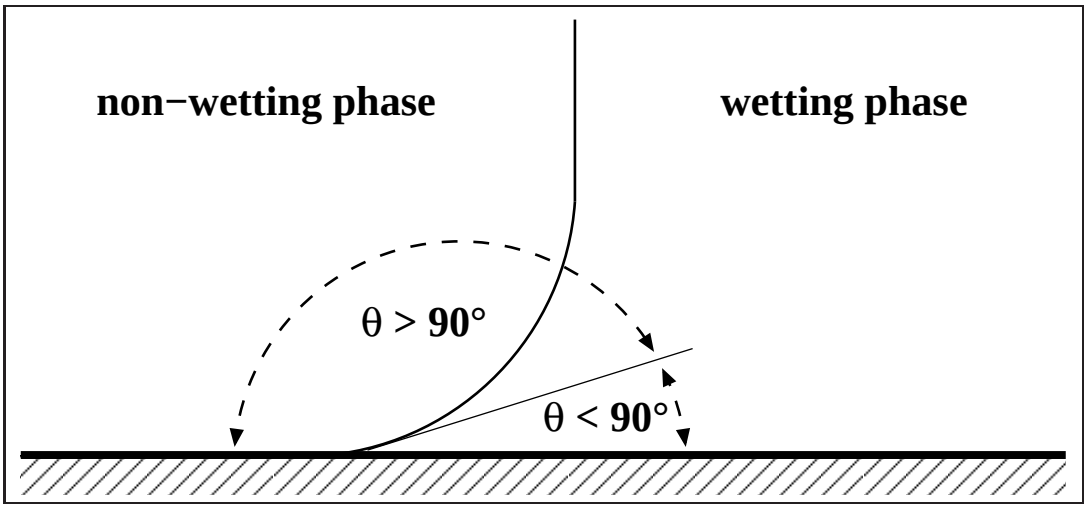

Fig. 6 Contact angle between a wetting and a non-wetting fluid.

the authors present an interface concept to couple two-phase flow processes in different types of porous media. The coupling of different models for one, two or three-phase flow incorporating an iterative non-linear solver to ensure the interface coupling conditions was presented in [108].

3 Mathematical models for flow and transport processes in porous media

We introduce the balance equations of flow and transport processes in porous media by means of an REV concept, i.e. on our fine scale. These equations may be upscaled in a subsequent step using one of the techniques of Section 2.2.1 or used in a multi-scale technique of Section 2.2.2. After establishing the necessary physical background, the equations for isothermal multi-phase flow processes are derived, both for the case of immiscible fluids as well as for miscible fluids. Furthermore, we give an introduction to different decoupled formulations of the balance equations paving the way for specialized solution schemes discussed in the following section. Finally, an extension to non-isothermal processes is provided.

3.1 Preliminaries

After stating the basic defintions of phases and components, the essential fluid and matrix parameters are introduced. Parameters and constitutive relations describing fluid-matrix interactions are discussed, and some common laws for fluid phase equilibria are reviewed.

3.1.1 Basic Definitions

Phases If two or more fluids fill a volume (e.g. the pore volume), are immiscible and separated by a sharp interface, each fluid is called a phase of the multi-phase system. Formally, the solid matrix can also be considered as a phase. If the solubility effects are not negligible, the fluid system has to be considered as a compositional multi-phase system.

A pair of two different fluid phases can be divided into a wetting and a non-wetting phase. Here, the important property is the contact angle θ between fluid-fluid interface and solid surface (Figure 6). If the contact angle is acute, the phase has a higher affinity to the solid and is therefore called wetting, whereas the other phase is called non-wetting.

Components A phase usually consists of several components which can either be pure chemical substances, or consist of several substances which form a unit with constant physical properties, such as air. Thus, it depends on the model problem which substances or mixtures of substances are considered as a component. The choice of the components is essential, as balance equations for compositional flow systems are in general formulated with respect to components.

3.1.2 Fluid Parameters

Compositions and concentrations The composition of a phase α is described by fractions of the different components contained in the phase. *Mass fractions* X_α^κ give the ratio of the mass m_κ of one component κ to the total mass of phase α,

$$X_\alpha^\kappa = \frac{m^\kappa}{\sum_\kappa m^\kappa}\,. \tag{1}$$

From this definition, it is obvious that the mass fractions sum up to unity for each phase,

$$\sum_\kappa X_\alpha^\kappa = 1. \tag{2}$$

A concept which is widely used in chemistry and thermodynamics, are *mole fractions* which phasewise relate the number of molecules of one component to the total number of components. Mole fractions are commonly denoted by lower case letters and can be calculated from mass fractions via the molar mass M^κ by

$$x_\alpha^\kappa = \frac{X_\alpha^\kappa / M^\kappa}{\sum_\kappa X_\alpha^\kappa / M^\kappa} \tag{3}$$

Both, mole fractions and mass fractions are dimensionless quantities. *Concentration* is the mass of a component per volume of the phase, and thus obtained by multiplying the mass fraction of the component by the density of the phase, $C_\alpha^\kappa = \varrho_\alpha X_\alpha^\kappa$, which yields the SI unit $\left[\mathsf{kg/m^3}\right]$.

Density The density ϱ relates the mass m of an amount of a substance to the volume V which is occupied by it:

$$\varrho = \frac{m}{V}. \tag{4}$$

The corresponding unit is $\left[\mathsf{kg/m^3}\right]$. For a fluid phase α, it depends on the phase pressure p_α and temperature T, as well as on the composition x_α^κ of the phase,

$$\varrho_\alpha = \varrho_\alpha(p_\alpha, T, x_\alpha^\kappa). \tag{5}$$

Since the compressibility of the solid matrix as well as its temperature-dependence can be neglected for many applications, one can often assign a constant density to solids.

For liquid phases, the dependence of density on the pressure is usually very low and the contribution by dissolved components is not significant. Thus, the density can be assumed to be only dependent on temperature, $\varrho_\alpha = \varrho_\alpha(T)$. For isothermal systems, the temperature is constant in time and thus, the density of the liquid phase is also constant in time.

The density of gases is highly dependent on temperature as well as on pressure.

Viscosity Viscosity is a measure for the resistance of a fluid to deformation under shear stress. For Newtonian fluids, the fluid shear stress τ is proportional to the temporal deformation of an angle γ, namely, $\tau = \mu\,\partial\gamma/\partial t$. The proportionality factor μ is called dynamic viscosity with the SI unit $\left[(\mathsf{N\cdot s})\,/\mathsf{m^2}\right] = \left[\mathsf{kg}/\left(\mathsf{m\cdot s}\right)\right]$. In general, the viscosity of liquid phases is primarily determined by their composition and by temperature. With increasing temperature, the viscosity of liquids decreases. Contrarily, the viscosity of gases increases with increasing temperature (see e.g. [10]).

3.1.3 Matrix Parameters

Porosity A porous medium consists of a solid matrix and the pores. The dimensionless ratio of the pore space within the REV to the total volume of the REV is defined as porosity ϕ,

$$\phi = \frac{\text{volume of pore space within the REV}}{\text{total volume of the REV}}. \tag{6}$$

If the solid matrix is assumed to be rigid, the porosity is constant and independent of temperature, pressure or other variables.

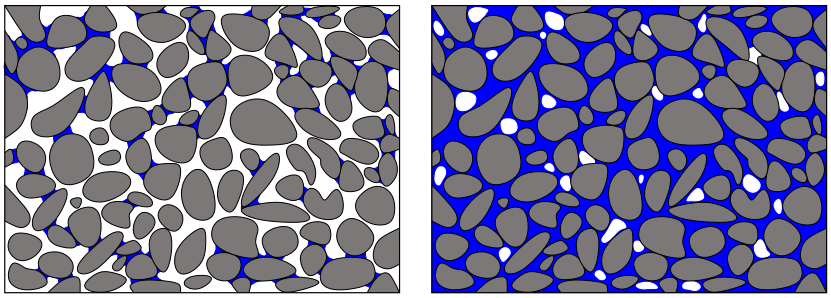

Fig. 7 Residual saturations of the wetting and non-wetting phase, respectively

Intrinsic Permeability The intrinsic permeability characterizes the inverse of the resistance of the porous matrix to flow through that matrix. Depending on the matrix type, the permeability may have different values for different flow directions which in general yields a tensor $\mathbf{K}$ with the unit $\left[\mathsf{m}^2\right]$.

3.1.4 Parameters Describing Fluid-Matrix Interaction

Saturation The pore space is divided and filled by the different phases. In the macroscopic approach (REV-scale), this is expressed by the saturation of each phase α. This dimensionless number is defined as the ratio of the volume of phase α within the REV to the volume of the pore space within the REV:

$$S_\alpha = \frac{\text{volume of phase } \alpha \text{ within the REV}}{\text{volume of the pore space within the REV}}. \tag{7}$$

Assuming that the pore space of the REV is completely filled by the fluid phases α, the sum of the phase saturations must be equal to one,

$$\sum_\alpha S_\alpha = 1. \tag{8}$$

If no phase transition occurs, the saturations change due to displacement of one phase by another phase. However, a phase can in general not be fully displaced by another, but a certian saturation will be held back, which is called *residual saturation* . For a wetting phase, a residual saturation occurs if parts of the displaced wetting phase are held back in the finer pore channels during the drainage process (see Figure 7, left hand side). On the other side, a residual saturation for the non-wetting phase may occur if bubbles of the displaced non-wetting phase are trapped by surrounding wetting phase during the imbibition process (see Figure 7, right hand side). Therefore, a residual saturation may depend on the pore geometry, the heterogeneity and the displacement process, but also on the number of drainage and imbibition cycles. If the saturation of a phase S_α is smaller than its residual saturation, the relative permeability (Section 3.1.4) of phase α is equal to zero which means that no flux of that phase can take place. This implies that a flux can only occur, if the saturation of a phase α lies between the residual saturation and unity ($S_{\mathrm{r}\alpha} \leq S_\alpha \leq 1$). With the residual saturation, an effective saturation for a two phase system can be defined in the following way:

$$S_{\mathrm{e}} = \frac{S_{\mathrm{w}} - S_{\mathrm{rw}}}{1 - S_{\mathrm{rw}}} \qquad S_{\mathrm{rw}} \leq S_{\mathrm{w}} \leq 1. \tag{9}$$

Alternatively, in many models the following definition is used:

$$S_{\mathrm{e}} = \frac{S_{\mathrm{w}} - S_{\mathrm{rw}}}{1 - S_{\mathrm{rw}} - S_{\mathrm{rn}}} \qquad S_{\mathrm{rw}} \leq S_{\mathrm{w}} \leq 1 - S_{\mathrm{rn}}. \tag{10}$$

Which definition has to be used, depends on the way the capillary pressure and the relative permeability curves are obtained, as explained below. Further considerations on the use of effective saturations are made in [68].

Capillarity Due to interfacial tension, forces occur at the interface of two phases. This effect is caused by interactions of the fluids on the molecular scale. Therefore, the interface between a wetting and a non-wetting phase is curved and the equilibrium at the interface leads to a pressure difference between the phases called capillary pressure p_c:

$$p_c = p_n - p_w, \tag{11}$$

where p_n is the non-wetting phase and p_w the wetting phase pressure. In a macroscopic consideration, an increase of the non-wetting phase saturation leads to a decrease of the wetting phase saturation, and, according to microscopic considerations, to the retreat of the wetting fluid to smaller pores. On the REV-scale, it is common to regard the macroscopic capillary pressure as a function of the saturation,

$$p_c = p_c(S_w), \tag{12}$$

the so-called capillary pressure-saturation relation. The simplest way to define a capillary pressure-saturation function is a linear approach:

$$p_c(S_e(S_w)) = p_{c,\max}(1 - S_e(S_w)). \tag{13}$$

The most common p_c-S_w-relations for a twophase system are those of Brooks and Corey and van Genuchten .

In the Brooks–Corey model,

$$p_c(S_e(S_w)) = p_d S_e(S_w)^{-\frac{1}{\lambda}} \qquad p_c \leq p_d, \tag{14}$$

the capillary pressure is a function of the effective Saturation S_e. The entry pressure p_d represents the minimum pressure needed for a non-wetting fluid to enter a porous medium initially saturated by a wetting fluid. The parameter λ is called pore-size distribution index and usually lies between 0.2 and 3.0. A very small λ-parameter describes a single size material, while a very large parameter indicates a highly non-uniform material.

The parameters of the Brooks–Corey relation are determined by fitting to experimental data. The effective saturation definition which is used in this parameter fitting is also the one to choose for later application of the respective capillary pressure or relative permeability function.

Relative Permeability Flow in porous media is strongly influenced by the interaction between the fluid phase and the solid phase. If more than one fluid phase fill the pore space, the presence of one phase also disturbs the flow behaviour of another phase. Therefore, the relative permeability $k_{r\alpha}$ which can be considered as a scaling factor is included into the permeability concept. Considering a two fluid phase system, the space available for one of the fluids depends on the amount of the second fluid within the system. The wetting phase, for example, has to flow around those parts of the porous medium occupied by non-wetting fluid, or has to displace the non-wetting fluid to find new flow paths. In a macroscopic view, this means that the cross-sectional area available for the flow of a phase is depending on its saturation. If the disturbance of the flow of one phase is only due to the restriction of available pore volume caused by the presence of the other fluid, a linear correlation for the relative permeability can be applied,

$$k_{rw}(S_e(S_w)) = S_e(S_w), \tag{15}$$

$$k_{rn}(S_e(S_w)) = 1 - S_e(S_w). \tag{16}$$

This formulation also implies that the relative permeability becomes zero if the residual saturation, representing the amount of immobile fluid, is reached.

In reality, one phase usually not only influences the flow of another phase just by the restriction in available volume, but also by additional interactions between the fluids. If capillary effects occur, the wetting phase, for example, fills the smaller pores if the saturation is small. This means that in case of an increasing saturation of the wetting phase, the relative permeability k_{rw} has to increase slowly if the saturations are still small and it has to increase fast if the saturations become higher, since then the wetting phase begins to fill the larger pores. For the non-wetting phase the opposite situation is the case. Increasing the saturation, the larger pores are filled at first causing a faster rise of k_{rn}. At higher saturations the smaller pores become filled which slows down the increase of the relative permeability. Therefore, correlations for the relative permeabilities can be defined using the

known capillary pressure-saturation relationships (details, see [68]). Besides capillary pressure effects also other effects might occur.

As an example, the Brooks–Corey model is defined as

$$k_{\mathrm{rw}}(S_{\mathrm{e}}(S_{\mathrm{w}})) = S_{\mathrm{e}}(S_{\mathrm{w}})^{\frac{2+3\lambda}{\lambda}}, \tag{17}$$

$$k_{\mathrm{rn}}(S_{\mathrm{e}}(S_{\mathrm{w}})) = (1 - S_{\mathrm{e}}(S_{\mathrm{w}}))^2 \left[1 - S_{\mathrm{e}}(S_{\mathrm{w}})^{\frac{2+\lambda}{\lambda}}\right], \tag{18}$$

where λ is the empirical constant from the Brooks–Corey $p_{\mathrm{c}}(S)$-relationship (Equation 14). These relative permeabilities do not sum up to unity as for the linear relationship. This is caused by the effects described before, and means that one phase is slowed down stronger by the other phase as it would be only due to the restricted volume available for the flow.

3.1.5 Extended Darcy's law

In a macroscopic treatment (we are on our fine scale) of porous media, Darcy's law, which was originally obtained experimentally for single phase flow, can be used to calculate averaged velocities using the permeability. For multi-phase systems, extended Darcy's law incorporating relative permeabilities is formulated for each phase (details, see [68, 115]):

$$\mathbf{v}_\alpha = \frac{k_{\mathrm{r}\alpha}}{\mu_\alpha}\mathbf{K}(-\nabla p_\alpha + \varrho_\alpha \mathbf{g}), \tag{19}$$

where $k_{\mathrm{r}\alpha}$ is the relative permeability dependent on saturation, and $\mathbf{K}$ the intrinsic permeability dependent on the porous medium, μ the dynamic fluid viscosity, p_α the phase pressure and ϱ_α the phase density, while $\mathbf{g}$ is the gravity vector. The mobility of a phase is defined as $\lambda_\alpha = k_{\mathrm{r}\alpha}/\mu_\alpha$. Note that in equation (19), the pressure in phase α is used which is important, since the pressure of different phases can differ due to capillarity. The product of the relative and the intrinsic permeability $k_{\mathrm{r}\alpha}\mathbf{K}$ is often called total permeability $\mathbf{K}_{\mathrm{t}}$ or effective permeability $\mathbf{K}_{\mathrm{e}}$.

3.1.6 Laws for Fluid Phase Equilibria

We give a short summary of common physical relationships, which govern the equilibrium state between fluid phases and thus, the mass transfer processes, i.e. the exchange of components between phases. While a variety of other relationships can be found in literature, only Dalton's law, Raoult's law, as well as Henry's law are treated here.

Dalton's Law Dalton's Law states that the total pressure of a gas mixture equals the sum of the pressures of the gases that make up the mixture, namely,

$$p_{\mathrm{g}} = \sum_\kappa p_{\mathrm{g}}^\kappa, \tag{20}$$

where p_{g}^κ is the pressure of a single component κ, the partial pressure, which is by definition the product of the mole fraction of the respective component in the gas phase and the total pressure of the gas phase, i.e.,

$$p_{\mathrm{g}}^\kappa = x_{\mathrm{g}}^\kappa p_{\mathrm{g}}. \tag{21}$$

Raoult's Law Raoult's law describes the lowering of the vapor pressure of a pure substance in a solution. It relates the vapor pressure of components to the composition of the solution under the simplifying assumption of an ideal solution. The relationship can be derived from the equality of fugacities, see Prausnitz et al. [110]. According to Raoult's law, the vapor pressure of a solution of component κ is equal to the vapor pressure of the pure substance times the mole fraction of component κ in phase α.

$$p_{\mathrm{g}}^\kappa = x_\alpha^\kappa p_{\mathrm{vap}}^\kappa \tag{22}$$

Here, p_{vap}^κ denotes the vapor pressure of pure component κ which is generally a function of temperature.

Henry's Law Henry's law is valid for ideally diluted solutions and ideal gases. It is especially used for the calculation of the solution of gaseous components in liquids. Considering a system with gaseous component κ, a linear relationship between the mole fraction x_α^κ of component κ in the liquid phase and the partial pressure p_g^κ of κ in the gas phase is obtained,

$$x_\alpha^\kappa = H_\alpha^\kappa p_\mathrm{g}^\kappa. \tag{23}$$

The parameter H_α^κ denotes the Henry coefficient of component κ in phase α, which is dependent on temperature, $H_\alpha^\kappa = H_\alpha^\kappa(T)$.

Figure 8 shows the range of applicability of both Henry's law and Raoult's law for a binary system, where component 1 is a component forming a liquid phase, e.g. water, and component 2 is a component forming a gaseous phase, e.g. air. One can see that for low mole fractions of component 2 in the system (small amounts of dissolved air in the liquid phase), Henry's law can be applied whereas for mole fractions of component 1 close to 1 (small amounts of vapor in the gas phase), Raoult's law is the appropriate description. In general, the solvent follows Raoult's law as it is present in excess, whereas the dissolved substance follows Henry's law as it is highly diluted.

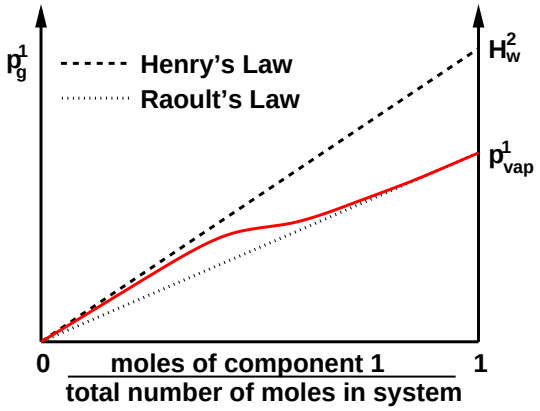

Fig. 8 Applicability of Henry's law and Raoult's law for a binary gas–liquid system (after Lüdecke and Lüdecke [91]).

3.1.7 The Reynolds transport theorem

A common way to derive balance equations in fluid dynamics is to use the Reynolds transport theorem, (e.g., [68, 136]), named after the British scientist Osborne Reynolds. Let E be an arbitrary property of the fluid (e.g., mass, energy, momentum) that can be obtained by the integration of a scalar field e over a moving control volume G,

$$E = \int_G e \,\mathrm{d}G\,. \tag{24}$$

The Reynolds transport theorem states that the temporal derivative of the property in a control volume moving with the fluid can be related to local changes of the scalar field by

$$\frac{\mathrm{d}E}{\mathrm{d}t} = \frac{\mathrm{d}}{\mathrm{d}t}\int_G e \,\mathrm{d}G = \int_G \left[\frac{\partial e}{\partial t} + \nabla\cdot(e\,\mathbf{v})\right]\mathrm{d}G\,, \tag{25}$$

For a general balance equation, we require a conservation of the property E. Thus the property can only change due to sinks and sources, diffusion or dissipation:

$$\frac{\mathrm{d}E}{\mathrm{d}t} = \int_G \frac{\partial e}{\partial t} + \nabla\cdot(e\mathbf{v})\,\mathrm{d}G = \int_G q^\mathrm{e} - \nabla\cdot\mathbf{w}\mathrm{d}G\,, \tag{26}$$

where $\mathbf{w}$ is the diffusive flux of e and q^e is the source per unit volume.

3.2 Multi-phase flow

We derive the mass balance equations for the immiscible and the miscible case. Both derivations are based on the general balance equation (26) and the insertion of extended Darcy's law (19) for the involved velocities.

3.2.1 The immiscible case

According to the specifications provided in Section 3.1, the mass of a phase α inside a control volume G can be expressed by

$$m_\alpha = \int_G \phi S_\alpha \varrho_\alpha \mathrm{d}G. \tag{27}$$

Under the assumption that the phases are immiscible, the total mass $m_\alpha = \int_G m_\alpha \mathrm{d}G$ is conserved, i.e. $\mathrm{d}m_\alpha/\mathrm{d}t = 0$ in the absence of external sources. Using the general balance equation (26), this mass conservation can be rewritten as

$$\int_G \frac{\partial\left(\phi\varrho_\alpha S_\alpha\right)}{\partial t} + \nabla\cdot\left(\phi S_\alpha \varrho_\alpha \mathbf{v}_{a\alpha}\right)\mathrm{d}G = \int_G \varrho_\alpha q_\alpha \mathrm{d}G\,. \tag{28}$$

We emphasize that the diffusive flux is assumed to be zero, since for the motion of phases on an REV scale, no diffusion or dispersion processes are considered. This, however, changes in the most upscaling approaches, where the loss of fine-scale informations is usually counterbalanced by dispersive fluxes on the coarse scale. The control volume considered for the transport theorem moves with $\mathbf{v}_{a\alpha}$, which is related to the Darcy velocity $\mathbf{v}_\alpha$ by

$$\mathbf{v}_\alpha = \phi S_\alpha \mathbf{v}_{a\alpha}. \tag{29}$$

Inserting (29) into (28) yields the integral balance equation for a single phase α in a multi-phase system

$$\int_G \frac{\partial\left(\phi\varrho_\alpha S_\alpha\right)}{\partial t} + \nabla\cdot\left(\varrho_\alpha \mathbf{v}_\alpha\right)\mathrm{d}G = \int_G \varrho_\alpha q_\alpha \mathrm{d}G\,, \tag{30}$$

Rewriting this equation in differential form and inserting extended Darcy's law (19) yields a system of n_α partial differential equations (with n_α the number of phases),

$$\frac{\partial\left(\phi\varrho_\alpha S_\alpha\right)}{\partial t} = -\nabla\cdot\left(\varrho_\alpha\lambda_\alpha\mathbf{K}\left(-\nabla p_\alpha + \varrho_\alpha\mathbf{g}\right)\right) + \varrho_\alpha q_\alpha. \tag{31}$$

Under isothermal conditions, the system (31) of n_α partial differential equations is already closed. In particular, the parameters ϕ, $\mathbf{K}$, $\mathbf{g}$ are intrinsic, and q_α are given source terms. The densities ϱ_α are functions of pressure and the known temperature only, and the mobilities λ_α only depend on the phase saturations. The remaining n_α constitutive relations for the $2n_\alpha$ unknowns S_α, p_α are the closure relation (8) and the $n_\alpha - 1$ capillary pressure-saturation relationships (12).

3.2.2 The miscible case

We now allow that each phase is made up of different components which can also be dissolved in the other phases. Inserting the total concentration per component,

$$C^\kappa = \phi\sum_\alpha \varrho_\alpha S_\alpha X_\alpha^\kappa, \tag{32}$$

into the general balance equation (26), and applying the same considerations on the velocities as in Section 3.2.1 yields

$$\int_G \frac{\partial C^\kappa}{\partial t} + \sum_\alpha \nabla\cdot\left(\varrho_\alpha X_\alpha^\kappa \mathbf{v}_\alpha\right)\mathrm{d}G = \int_G q^\kappa \mathrm{d}G\,, \tag{33}$$

Rewriting this in differential form and inserting the extended Darcy law (19), we obtain a set of n_κ partial differential equations (with n_κ the number of components),

$$\frac{\partial C^\kappa}{\partial t} = -\sum_\alpha \nabla \cdot (\varrho_\alpha X_\alpha^\kappa \lambda_\alpha \mathbf{K} (-\nabla p_\alpha + \varrho_\alpha \mathbf{g})) + q^\kappa. \tag{34}$$

We remark that the immiscible case (31) can be easily derived from (34) as a special case. In particular, immiscibility can be equally expressed as X_α^κ being known and constant with respect to space and time. By eventually regrouping and renaming the components with respect to the fixed phase compositions, we can furthermore assume that each component is associated with a distinct phase and $X_\alpha^\kappa = 1$ holds for this particular phase α, whereas it equals zero for all other phases. This directly leads to (31).

In general, we are left with n_κ partial differential equations (34) for the $2n_\alpha + n_\kappa \cdot n_\alpha$ unknowns $p_\alpha, S_\alpha, X_\alpha^\kappa$. Considering (8) and (12) as in the immiscible case, and additionally the closure relations (2), yields $2n_\alpha$ constraints. The remaining $n_\kappa(n_\alpha - 1)$ constraints have to be carefully chosen from the laws for fluid phase equilibria, see Section 3.1.6.

3.3 Decoupled Formulations

It is often advantageous to reformulate the mass balance equations (31) or (34) into one elliptic or parabolic equation for the pressure and one or more hyperbolic-parabolic transport equations for the saturations or concentrations, respectively. In particular, this reformulation allows to employ multi-scale or discretization approaches which are especially developed and suited for the corresponding type of equation, and to combine them in various ways. Furthermore, a sequential or iterative solution procedure reduces the amount of unknowns in each solution step. In the following, we introduce these decoupled formulations for the immiscible and for the miscible case.

3.3.1 The immiscible case

The reformulation of the multi-phase mass balance equations (31) into one pressure equation and one or more saturation equations was primarily derived in [27], where the author just called it *a new formulation* for two-phase flow in porous media. Due to the introduction of the idea of fractional flows this formulation is usually called fractional flow formulation.

Pressure Equation A pressure equation can be derived by addition of the phase mass balance equations. After some reformulation, a general pressure equation can be written as follows:

$$\sum_\alpha S_\alpha \frac{\partial \phi}{\partial t} + \nabla \cdot \mathbf{v}_\mathrm{t} + \sum_\alpha \frac{1}{\varrho_\alpha} \left[\phi S_\alpha \frac{\partial \varrho_\alpha}{\partial t} + \mathbf{v}_\alpha \cdot \nabla \varrho_\alpha \right] - \sum_\alpha q_\alpha = 0, \tag{35}$$

with the following definition of a total velocity:

$$\mathbf{v}_\mathrm{t} = \sum_\alpha \mathbf{v}_\alpha. \tag{36}$$

Inserting extended Darcy's law (19) into (36) yields

$$\mathbf{v}_\mathrm{t} = -\lambda_\mathrm{t} \mathbf{K} \left[\sum_\alpha f_\alpha \nabla p_\alpha - \sum_\alpha f_\alpha \varrho_\alpha \mathbf{g} \right]. \tag{37}$$

where $f_\alpha = \lambda_\alpha / \lambda_\mathrm{t}$ is the fractional flow function of phase α and $\lambda_\mathrm{t} = \sum_\alpha \lambda_\alpha$ is the total mobility. In the following, different possibilities to reformulate this general pressure equation for two-phase flow are shown. There also exist fractional flow approaches for three phases, which are not further considered here. For details, we exemplarily refer to [124].

Global Pressure Formulation for Two-Phase Flow Defining a global pressure p such that $\nabla p = \sum_\alpha f_\alpha \nabla p_\alpha$ (see below), equation (37) can be rewritten as a function of p:

$$\mathbf{v}_\mathrm{t} = -\lambda_\mathrm{t}\mathbf{K}\left[\nabla p - \sum_\alpha f_\alpha \varrho_\alpha \mathbf{g}\right] \tag{38}$$

Inserting (38) into (35) yields the pressure equation related to the global pressure.

For a domain Ω with boundary $\Gamma = \Gamma_\mathrm{D} \cup \Gamma_\mathrm{N}$, where Γ_D denotes a Dirichlet and Γ_N a Neumann boundary, the boundary conditions are:

$$\begin{array}{lllll} p & = p_\mathrm{D} & \text{on} & \Gamma_\mathrm{D} & \text{and} \\ \mathbf{v}_\mathrm{t}\cdot\mathbf{n} & = q_\mathrm{N} & \text{on} & \Gamma_\mathrm{N}. & \end{array} \tag{39}$$

This means that a global pressure has to be found on a Dirichlet boundary which can lead to problems, as the global pressure is no physical variable and thus can not be measured directly. Following [28], the global pressure is defined by

$$p = \frac{1}{2}\left(p_\mathrm{w} + p_\mathrm{n}\right) - \int_{S_\mathrm{c}}^{S_\mathrm{w}} \left(f_\mathrm{w}(S_\mathrm{w}) - \frac{1}{2}\right) \frac{\mathrm{d}p_\mathrm{c}}{\mathrm{d}S_\mathrm{w}}(S_\mathrm{w})\,\mathrm{d}S_\mathrm{w}, \tag{40}$$

where S_c is the saturation satisfying $p_\mathrm{c}(S_\mathrm{c}) = 0$. This definition makes sure that the global pressure is a smooth function and thus is easier to handle from a numerical point of view. However, as shown e.g. in [19], an iterative solution technique is required for more complex (realistic) conditions, where a phase pressure might be known at a boundary. It becomes also clear, that $p = p_\mathrm{w} = p_\mathrm{n}$, if the capillary pressure between the phases is neglected.

Phase Pressure Formulation for Two-Phase Flow A pressure equation can also be further derived using a phase pressure which is a physically meaningful parameter in a multi-phase system. Investigations of a phase pressure fractional flow formulation can for example be found in [34] and a formulation including phase potentials has been used in [71].

Exploiting equation (11), equation (37) can be rewritten in terms of one phase pressure. This yields a total velocity in terms of the wetting phase pressure as:

$$\mathbf{v}_\mathrm{t} = -\lambda_\mathrm{t}\mathbf{K}\left[\nabla p_\mathrm{w} + f_\mathrm{n}\nabla p_\mathrm{c} - \sum_\alpha f_\alpha \varrho_\alpha \mathbf{g}\right], \tag{41}$$

and in terms of a non-wetting phase pressure as:

$$\mathbf{v}_\mathrm{t} = -\lambda_\mathrm{t}\mathbf{K}\left[\nabla p_\mathrm{n} - f_\mathrm{w}\nabla p_\mathrm{c} - \sum_\alpha f_\alpha \varrho_\alpha \mathbf{g}\right], \tag{42}$$

Substituting $\mathbf{v}_t$ in the general pressure equation (35) by equation (41) or (42) yields the pressure equations as function of a phase pressure.

In analogy to the global pressure formulation, the following boundary conditions can be defined:

$$\begin{array}{lllll} p_\mathrm{w} & = p_\mathrm{D} & \text{on} & \Gamma_\mathrm{D} & \text{or} \\ p_\mathrm{n} & = p_\mathrm{D} & \text{on} & \Gamma_\mathrm{D} & \text{and} \\ \mathbf{v}_\mathrm{t}\cdot\mathbf{n} & = q_\mathrm{N} & \text{on} & \Gamma_\mathrm{N}. & \end{array} \tag{43}$$

It is important to point out that we now have a physically meaningful variable, the phase pressure, instead of the global pressure. So boundary conditions at Dirichlet boundaries can be defined directly, if a phase pressure at a boundary is known.

Saturation Equation We derive the transport equation for the saturation depending on whether a global or a phase pressure formulation is used. In the first case, a possibly degenerated parabolic-hyperbolic equation is derived, which is quite weakly coupled to the pressure equation. In the second case, a purely hyperbolic equation is obtained with a stronger coupling to the corresponding pressure equation.

Global Pressure formulation for Two-Phase Flow In the case of a global pressure formulation a transport equation for saturation related to the total velocity $\mathbf{v}_t$ has to be derived from the general multi-phase mass balance equations (35). With the definition of the capillary pressure (11), the extended Darcy's law (19) can be formulated for a wetting and a non-wetting phase as:

$$\mathbf{v}_\mathrm{w} = -\lambda_\mathrm{w}\mathbf{K}(\nabla p_\mathrm{w} - \varrho_\mathrm{w}\mathbf{g}) \tag{44}$$

and

$$\mathbf{v}_\mathrm{n} = -\lambda_\mathrm{n}\mathbf{K}(\nabla p_\mathrm{w} + \nabla p_\mathrm{c} - \varrho_\mathrm{w}\mathbf{g}). \tag{45}$$

Solving (45) for $\mathbf{K}\nabla p_\mathrm{w}$ and inserting it into Equation (44) yields:

$$\mathbf{v}_\mathrm{w} = \frac{\lambda_\mathrm{w}}{\lambda_\mathrm{n}}\mathbf{v}_\mathrm{n} + \lambda_\mathrm{w}\mathbf{K}[\nabla p_\mathrm{c} + (\varrho_\mathrm{w} - \varrho_\mathrm{n})\mathbf{g}]. \tag{46}$$

With $\mathbf{v}_\mathrm{n} = \mathbf{v}_\mathrm{t} - \mathbf{v}_\mathrm{w}$, (46) can be reformulated as the fractional flow equation for $\mathbf{v}_\mathrm{w}$:

$$\mathbf{v}_\mathrm{w} = \frac{\lambda_\mathrm{w}}{\lambda_\mathrm{w} + \lambda_\mathrm{n}}\mathbf{v}_\mathrm{t} + \frac{\lambda_\mathrm{w}\lambda_\mathrm{n}}{\lambda_\mathrm{w} + \lambda_\mathrm{n}}\mathbf{K}[\nabla p_\mathrm{c} + (\varrho_\mathrm{w} - \varrho_\mathrm{n})\mathbf{g}], \tag{47}$$

which can be further inserted into the wetting phase mass balance equation leading to a transport equation for the wetting phase saturation related to $\mathbf{v}_\mathrm{t}$:

$$\frac{\partial(\phi\varrho_\mathrm{w}S_\mathrm{w})}{\partial t} + \nabla\cdot[\varrho_\mathrm{w}(f_\mathrm{w}\mathbf{v}_\mathrm{t} + f_\mathrm{w}\lambda_\mathrm{n}\mathbf{K}(\nabla p_\mathrm{c} + (\varrho_\mathrm{w} - \varrho_\mathrm{n})\mathbf{g}))] - \varrho_\mathrm{w}q_\mathrm{w} = 0. \tag{48}$$

Some terms of (48) can be reformulated in dependence on the saturation (details, see [68]). For incompressible fluids and a porosity which does not change in time, the saturation equation of a two-phase system can then be formulated showing the typical character of a transport equation as

$$\begin{aligned}\phi\frac{\partial S_\mathrm{w}}{\partial t} + \left[\mathbf{v}_\mathrm{t}\frac{\mathrm{d}f_\mathrm{w}}{\mathrm{d}S_\mathrm{w}} + \frac{\mathrm{d}\,(f_\mathrm{w}\lambda_\mathrm{n})}{\mathrm{d}S_\mathrm{w}}\mathbf{K}(\varrho_\mathrm{w} - \varrho_\mathrm{n})\mathbf{g}\right]\cdot\nabla S_\mathrm{w} \\ +\nabla\cdot\left[\bar{\lambda}\mathbf{K}\frac{\mathrm{d}p_\mathrm{c}}{\mathrm{d}S_\mathrm{w}}\nabla S_\mathrm{w}\right] - q_\mathrm{w} + f_\mathrm{w}q_\mathrm{t} = 0,\end{aligned} \tag{49}$$

where $q_\mathrm{t} = q_\mathrm{w} + q_\mathrm{n}$.

Similarly, an equation for the non-wetting phase saturation can be derived which can be written in its final form as:

$$\frac{\partial(\phi\varrho_\mathrm{n}S_\mathrm{n})}{\partial t} + \nabla\cdot[\varrho_\mathrm{n}(f_\mathrm{n}\mathbf{v}_\mathrm{t} - f_\mathrm{n}\lambda_\mathrm{w}\mathbf{K}(\nabla p_\mathrm{c} - (\varrho_\mathrm{n} - \varrho_\mathrm{w})\mathbf{g}))] - \varrho_\mathrm{n}q_\mathrm{n} = 0. \tag{50}$$

Phase Pressure Formulation for Two-Phase Flow Obviously, for the phase pressure formulation the saturation can be calculated directly from the mass balance equations (35), leading to

$$\frac{\partial\,(\phi\varrho_\mathrm{w}S_\mathrm{w})}{\partial t} + \nabla\cdot(\varrho_\mathrm{w}\mathbf{v}_\mathrm{w}) = q_\mathrm{w} \tag{51}$$

for the wetting phase of a two-phase system and to

$$\frac{\partial\,(\phi\varrho_\mathrm{n}S_\mathrm{n})}{\partial t} + \nabla\cdot(\varrho_\mathrm{n}\mathbf{v}_\mathrm{n}) = q_\mathrm{n}, \tag{52}$$

where the phase velocities can be calculated using extended Darcy's law.

A nice feature of the global pressure formulation is that the two equations (pressure equation and saturation equation) are only weakly coupled through the presence of the total mobility and the fractional flow functions in the pressure equation. These are dependent on the relative permeabilities of the phases and thus dependent on the saturation. This also holds for the phase pressure formulation. However, in this formulation the coupling is strengthened again due to the additional capillary pressure term in the pressure equation.

3.3.2 The miscible case

Similarly to the fractional flow formulations for immiscible multi-phase flow, decoupled formulations for compositional flow have been developed. However, dissolution and phase changes of components affect the volume of mixtures, compromising the assumption of a divergence-free total velocity field. In [126], a pressure equation for compositional flow in porous media based on volume conservation is presented. The basic and physically logical constraint of this equation is that the pore space always has to be filled by some fluid i.e., the volume of the fluid mixture has to equal the pore volume. Using a similar definition as for component mass fractions in Section 3.1.2, each phase can be assigned a mass fraction that relates the mass of the phase to the mass of all phases present in the control volume and can be related to saturations by $\nu_\alpha = S_\alpha \varrho_\alpha / \sum_\alpha S_\alpha \varrho_\alpha$. Knowing the total mass $m_t = \sum_\alpha S_\alpha \varrho_\alpha = \sum_\kappa C^\kappa$ (with the unit $\left[\mathsf{kg/m^3}\right]$ and C^κ as defined in Section 3.2.2) of a mixture inside a control volume and the phase mass fraction ν_α, we can calculate the volume occupied by the phase by $v_\alpha = m_t \nu_\alpha / \varrho_\alpha$. Related to a unit volume, the pore volume is the porosity ϕ and the total mass of a mixture is the sum over the total concentrations and thus the constraint stated above can be expressed as:

$$\left(\sum_\kappa C^\kappa \right) \cdot \left(\sum_\alpha \frac{\nu_\alpha}{\varrho_\alpha} \right) = \phi \, . \tag{53}$$

Since the fluid volume v_t, which is defined by the left hand side of equation (53) always has to fill the pore volume it is not allowed to change, i.e.

$$\frac{\partial v_\mathrm{t}}{\partial t} = 0 \, . \tag{54}$$

However, the fluid volume changes due to changes in the composition of the mixture and due to changes in pressure, which can be expressed by derivatives of the volume with respect to pressure and total concentration. These changes have to be compensated by inflow or outflow of mass to or from the control volume which, according to [126] or [32], can be expressed by the pressure equation for compositional flow:

$$-\frac{\partial v_\mathrm{t}}{\partial p}\frac{\partial p}{\partial t} + \sum_\kappa \frac{\partial v_\mathrm{t}}{\partial C^\kappa} \nabla \cdot \sum_\alpha X_\alpha^\kappa \varrho_\alpha \mathbf{v}_\alpha = \sum_\kappa \frac{\partial v_\mathrm{t}}{\partial C^\kappa} q^\kappa \, . \tag{55}$$

In [32], the authors show a more detailed derivation and also introduce and analyze the fractional flow formulation in terms of phase pressure, weighted phase pressure and global pressure. However, in this publication, we remain at calculating the phase velocities with extended Darcy's law (equation (19)) without introducing fractional flows, since – in the opinion of the authors – this is the most convenient.

3.4 Non-isothermal flow

The consideration of non-isothermal flow processes involves an additional conservation property: energy. This is expressed as internal energy inside a unit volume which consists of the internal energies of the matrix and the fluids:

$$U = \int_G \phi \sum_\alpha \left(\varrho_\alpha S_\alpha u_\alpha \right) + \left(1 - \phi \right) \varrho_\mathrm{s} c_\mathrm{s} T \, \mathrm{d}G \, , \tag{56}$$

where the internal energy is assumed to be a linear function of temperature T above a reference point. Then c_s denotes the heat capacity of the rock and u_α is the specific internal energy of phase α. The internal energy in a system is increased by heat fluxes into the system and by mechanical work done on the system

$$\frac{\mathrm{d}U}{\mathrm{d}t} = \frac{\mathrm{d}Q}{\mathrm{d}t} + \frac{\mathrm{d}W}{\mathrm{d}t} \, . \tag{57}$$

Heat flows over the control volume boundaries by conduction, which is a linear function of the temperature gradient and occurs in direction of falling temperatures

$$\frac{\mathrm{d}Q}{\mathrm{d}t} = \oint_\Gamma -\mathbf{n} \cdot \left(-\lambda_\mathrm{s} \nabla T \right) \mathrm{d}\Gamma = \int_G \nabla \cdot \left(\lambda_\mathrm{s} \nabla T \right) \mathrm{d}G \, . \tag{58}$$

The mechanical work done by the system (and therefore decreasing its energy) is volume changing work. It is done when fluids flows over the control volume boundaries against a pressure p

$$\frac{\mathrm{d}W}{\mathrm{d}t} = \oint_\Gamma -p\,(\mathbf{n}\cdot\mathbf{v})\,\mathrm{d}\Gamma = \int_G -\nabla\cdot(p\mathbf{v})\,\mathrm{d}G\,. \tag{59}$$

The left hand side of equation (57) can be expressed by the Reynolds transport theorem, where the velocity of the solid phase equals zero

$$\begin{aligned}\frac{\mathrm{d}U}{\mathrm{d}t} = &\int_G \frac{\partial}{\partial t}\left(\phi\sum_\alpha(\varrho_\alpha S_\alpha u_\alpha)\right) + \frac{\partial}{\partial t}\left((1-\phi)\,\varrho_\mathrm{s}c_\mathrm{s}T\right)\mathrm{d}G\\ &+\oint_\Gamma \mathbf{n}\cdot\sum_\alpha(\varrho_\alpha u_\alpha\mathbf{v}_\alpha)\,\mathrm{d}\Gamma\,.\end{aligned} \tag{60}$$

Using the definition of specific enthalpy $h = u + p/\varrho$, the second term on the right hand side of equation (60) and the right hand side of equation (59) can be combined and equation (57) can be rewritten to

$$\begin{aligned}&\int_G \frac{\partial}{\partial t}\left(\phi\sum_\alpha(\varrho_\alpha S_\alpha u_\alpha)\right) + \frac{\partial}{\partial t}\left((1-\phi)\,\varrho_\mathrm{s}c_\mathrm{s}T\right)\mathrm{d}G\\ &= \oint_\Gamma \mathbf{n}\cdot(\lambda_\mathrm{s}\nabla T)\,\mathrm{d}\Gamma - \oint_\Gamma \mathbf{n}\cdot\sum_\alpha(\varrho_\alpha h_\alpha\mathbf{v}_\alpha)\,\mathrm{d}\Gamma\end{aligned} \tag{61}$$

or in differential form

$$\begin{aligned}&\frac{\partial}{\partial t}\left(\phi\sum_\alpha(\varrho_\alpha S_\alpha u_\alpha)\right) + \frac{\partial}{\partial t}\left((1-\phi)\,\varrho_\mathrm{s}c_\mathrm{s}T\right)\\ &= \nabla\cdot(\lambda_\mathrm{s}\nabla T) - \nabla\cdot\sum_\alpha(\varrho_\alpha h_\alpha\mathbf{v}_\alpha)\end{aligned} \tag{62}$$

4 Numerical solution approaches

After establishing the continuous models, it remains to choose numerical discretization and solution schemes. We will only very briefly address this question for the fully coupled balance equations (31) or (34) in Section 4.1, our main emphasis here is on the decoupled systems, which will be treated in Section 4.2.

4.1 Solution of the fully coupled equations

One possibility to calculate multi-phase flow is to directly solve the system of equations given by the balances (31) or (34). These mass balance equations are usually non-linear and strongly coupled. Thus, we also call this the fully coupled multi-phase flow formulation. After space discretization, the system of equations one has to solve can be written as:

$$\frac{\partial}{\partial t}\mathbf{M}(\underline{u}) + \mathbf{A}(\underline{u}) = \mathbf{R}(\underline{u}), \tag{63}$$

where $\mathbf{M}$ consists of the accumulation terms, $\mathbf{A}$ includes the internal flux terms and $\mathbf{R}$ is the right hand side vector which comprises Neumann boundary flux terms as well as source or sink terms. All mass balance equations have to be solved simultaneously due to the strong coupling. Therefore, a linearization technique has to be applied. The most common solution method is the Newton-Raphson-algorithm [12, 42].

Advantages of the fully coupled formulation and the implicit method respectively are that it includes the whole range of physical effects (capillarity, gravity,...) without having additional effort; that it is quite stable; and that it is usually not very sensitive to the choice of the time step size. The disadvantage

is that a global system of equations, which is twice as large as for a single phase pressure equation if two-phase flow is calculated (and even larger in the non-isothermal case or including more phases), has to be solved *several* times during each time step, dependent on the number of iterations the linearization algorithm needs to converge.

4.2 Solution of the decoupled equations

As before, we split our considerations into the immiscible and the miscible case.

4.2.1 The immiscible case

As their name implies, decoupled formulations decouple the system of equations of a multi-phase flow formulation to some extent. In the immiscible case, the result is an equation for pressure and additional transport equations for one saturation (see Section 3.3.1) in the case of two-phase flow or several saturations if more phases are considered. The new equations are still weakly coupled due to the saturation dependent parameters like relative permeabilities or capillary pressure in the pressure equation and the pressure dependent parameters like density and viscosity in the saturation transport equation. Nevertheless, in many cases it is possible to solve this system of equations sequentially. Numerically, this is usually done by using an IMPES scheme (IMplicit Pressure - Explicit Saturation), which was first introduced in [117, 122]. Therefore, the pressure equation is solved first implicitly. From the resulting pressure field the velocity field can be calculated and inserted into the saturation equation which is then solved explicitly.

One major advantage of the decoupled formulation is that it allows for different discretizations of the different equations. For the pressure equation, it is of utmost importance that its solution admits the calculation of a locally conservative velocity field. There are various discretization methods meeting this requirement, like finite volumes with two-point or multi-point flux approximation, [3, 4, 25, 55, 87], mixed finite elements, [7, 21, 74, 96, 120], or mimetic finite differences, [18, 22, 23, 77, 116]. Moreover, it is also possible to use discretizations with non-conservative standard velocity fields, and employ a post-processing step to reconstruct a locally conservative scheme. This has been investigated for discontinuous Galerkin methods in [16], while for standard Lagrangian finite elements, it is possible to calculate equilibrated fluxes known from a posteriori error estimation, [5].

For the solution of the transport equation(s) also exists a large variety of discretization possibilities, ranging from standard upwind finite volume approaches, [59, 90], over higher order discontinuous Galerkin methods with slope limiter, [36, 37, 61, 70], the modified method of characteristics, [31, 41, 45, 56], and the Eulerian-Lagrangian localized adjoint method, [57, 58, 69, 113, 132], up to streamline methods [84, 95, 105].

The IMPES scheme can be very efficient, since a system of equations with only n unknowns, where n is the number of degrees of freedom for the discretization of the pressure equation, has to be solved only once in the pressure step, as opposed to several solutions of a system of equations with m unknowns in the fully coupled scheme, where m is usually at least twice as large as n. However, there are strong restrictions with respect to the choice of the time step size. In a multi-dimensional advection dominated porous media flow a time step criterion can be defined as follows:

$$\Delta t_{\text{in}} = \frac{V}{|\int\limits_{\Gamma} \sum\limits_{\alpha} (\mathbf{v}_{\alpha_{\text{in}}} \cdot \mathbf{n})\, d\Gamma|} \tag{64}$$

$$\Delta t_{\text{out}} = \frac{V}{|\int\limits_{\Gamma} \sum\limits_{\alpha} (\mathbf{v}_{\alpha_{\text{out}}} \cdot \mathbf{n})\, d\Gamma|} \tag{65}$$

$$\Delta t \leq a \, \min(\Delta t_{\text{in}}, \Delta t_{\text{out}}) \tag{66}$$

where V is the volume within a cell available for the flow, $\mathbf{v}_{\alpha_{\text{in}}}$ is a phase velocity causing flux into a cell, and $\mathbf{v}_{\alpha_{\text{out}}}$ is a phase velocity causing flux out of a cell. To capture the non-linear character of two-phase flow it might be necessary to strengthen the time-step restriction. This can be done by choosing a suitable a, where $0 < a \leq 1$. The value of a can either be found heuristically or by a

calculation taking into account some more detailed analysis of the non-linear behavior (e.g, see [11]). In the one-dimensional linear case where $a = 1$, equations (64), (65) and (66) lead to

$$\Delta t \leq \min\left(\frac{\Delta x}{|\sum_{\alpha} \mathbf{v}_{\alpha_{\text{in}}}|}, \frac{\Delta x}{|\sum_{\alpha} \mathbf{v}_{\alpha_{\text{out}}}|}\right), \tag{67}$$

which is the well-known Courant–Friedrichs–Lewy CFL-condition. Detailed analysis of the stability of an IMPES scheme can be found in [11]. There is also shown that the time step size is further restricted if the flow is dominated by diffusive effects. An explicit scheme may then lose its efficiency compared to an implicit scheme, as a large number of time steps can be required. A comparison between an IMPES scheme and an fully implicit scheme can for example be found in [118].

4.2.2 The compositional case

The decoupled compositional multi-phase flow equations derived in Section 3.3.2 can be solved sequentially according to the IMPES scheme, where it is commonly referred to as IMPEC scheme, since concentrations are considered in this case. First, the pressure equation (55) is solved implicitly to obtain a pressure field and fluid phase velocities which are used to explicitly solve the transport equation (34). After each of these pressure-transport sequences, the distribution of total concentrations is known. For the next sequence, phase saturation and component mass fractions are needed. These are gained by performing a phase equilibrium- or so-called flash calculation (see below), which forms the last step of the IMPEC scheme.

Flash calculations After the evaluation of the transport equation, the total concentrations at each cell or node are known. From these, an overall mass fraction (or feed mass fraction) $z^\kappa = C^\kappa / \sum_\kappa C^\kappa$ of each component inside the mixture is calculated. Now the question is, how the phase mass fractions ν_α can be calculated from this, i.e. how the different components are distributed among the different phases. Therefore, we introduce at first the equilibrium ratios

$$K_\alpha^\kappa = \frac{X_\alpha^\kappa}{X_\text{r}^\kappa}\,, \tag{68}$$

which relate the mass fractions of each component in each phase α to its mass fraction in a reference phase r, where K_r^κ obviously always equals unity. The equilibrium ratios can be obtained by using the laws for fluid phase equilibria in section 3.1.6, as described in [101] or by incorporating a thermodynamic equation of state [12, 97, 99]. In the former case, the equilibrium ratios depend only on pressure and are therefore constant for constant pressure and temperature. The feed mass fraction z^κ can be related to the phase mass fractions X_α^κ by

$$z^\kappa = \sum_\alpha \nu_\alpha X_\alpha^\kappa\,. \tag{69}$$

Combining and rearranging of (68) and (69) yields

$$X_\text{r}^\kappa = \sum_\kappa \frac{z^\kappa}{\sum\limits_{\alpha \neq \text{r}} K_\alpha^\kappa \nu_\alpha + \nu_\text{r}}, \tag{70}$$

and some more steps, which are elaborately described in [12], yield a set of $n_\alpha - 1$ equations, known as the Rachford-Rice equation

$$\sum_\kappa \frac{z^\kappa \left(K_\alpha^\kappa - 1\right)}{1 + \sum\limits_{\alpha \neq \text{r}} \left(K_\alpha^\kappa - 1\right) \nu_\alpha} = 0 \qquad \forall \alpha \neq \text{r}\,, \tag{71}$$

which generally has to be solved iteratively for the phase mass fraction ν_α. Only in the case of the same number of phases and components, the Rachford–Rice equation can be solved analytically. Once the phase mass fractions are known, the mass fractions of the components inside the reference phase can be calculated by (70) and then lead to the mass fractions inside the other phases via (68). Other flash calculation approaches which use so-called reduced equation algorithms and which basically use modified forms of the presented equations are presented in [133].

5 Application of multi-physics and multi-scale methods

Unlike numerical multi-scale methods, our ideology is to use a physically based multi-scale multi-physics method that uses physical indicators to identify the domains where different processes take place. The idea in mind is always to create a tool which is able to handle complex real-life application. Therefore, the coupling of scales and domains is done in a physically motivated way, e.g. by ensuring continuity of fluxes and pressures across domain boundaries.

5.1 A multi-physics example

In this section, we introduce a method to couple compositional two-phase flow with single-phase compositional flow as proposed in [60].The advantage of this coupling is, that for single-phase compositional flow, a simpler pressure equation and only one transport equation have to be solved. Moreover, for single-phase flow, the evaluation of flash calculations can be avoided. This is interesting if these evaluations require lots of computational power such as in many reservoir engineering problems, where flash calculations may occupy up to 70 % of the total CPU time of a model (see [121]).

5.1.1 Single phase transport

We want to take a closer look at the equations for the miscible case and assume that only one phase is present. Inserting the definition of the total concentration (32) into the component mass balance equation (34) for one phase α and applying the chain rule yields

$$\phi \varrho_\alpha X_\alpha^\kappa \frac{\partial S_\alpha}{\partial t} + S_\alpha \varrho_\alpha X_\alpha^\kappa \frac{\partial \phi}{\partial t} + \phi S_\alpha \varrho_\alpha \frac{\partial X_\alpha^\kappa}{\partial t} = -\nabla \cdot (\mathbf{v}_\alpha \varrho_\alpha X_\alpha^\kappa) + q^\kappa \, . \tag{72}$$

The first term on the left hand side equals zero since only one phase is present and thus the saturation always equals unity. Further we assume that phase and matrix compressibilities are of low importance and can be neglected. Then the second and third term on the left hand side cancel out as well. A volumetric source q_α of the present phase with the composition X_Q^κ is introduced and using the definition $q^\kappa = q_\alpha \varrho_\alpha X_Q^\kappa$, with X_Q^κ in the source-flow, we replace the mass source of component κ and write

$$\phi \varrho_\alpha \frac{\partial X_\alpha^\kappa}{\partial t} = \frac{\partial C^\kappa}{\partial t} = -\varrho_\alpha \nabla \cdot (\mathbf{v}_\alpha X_\alpha^\kappa) + q_\alpha \varrho_\alpha X_Q^\kappa \, . \tag{73}$$

This is the mass balance equation for the compositional transport in a single phase. The same assumptions can be applied to the compositional pressure equation. For incompressible flow, the derivatives of volume with respect to mass equal the reciprocal of the phase density, i.e. $\partial v_\mathrm{t} / \partial C^\kappa = 1/\varrho_\alpha$. Inserting this identity into equation (55), setting the derivative of volume with respect to pressure to zero (incompressible flow) and applying the chain rule to the divergence term, we get

$$\sum_\kappa \frac{1}{\varrho_\alpha} \left(X_\alpha^\kappa \varrho_\alpha \nabla \cdot \mathbf{v}_\alpha + \varrho_\alpha \mathbf{v}_\alpha \cdot \nabla X_\alpha^\kappa + X_\alpha^\kappa \mathbf{v}_\alpha \cdot \nabla \varrho_\alpha \right) = \sum_\kappa \frac{1}{\varrho_\alpha} q^\kappa \, . \tag{74}$$

By definintion, the sum of the mass fractions X_α^κ inside one phase equals unity, thus the second term in parenthesis cancels out. Furthermore, the gradient of the density equals zero due to the incompressibility. Again introducing the volumetric source term as above, yields the pressure equation for incompressible single phase compositional flow, which can as well be derived from equation (35):

$$\nabla \cdot \mathbf{v}_\alpha = q_\alpha \tag{75}$$

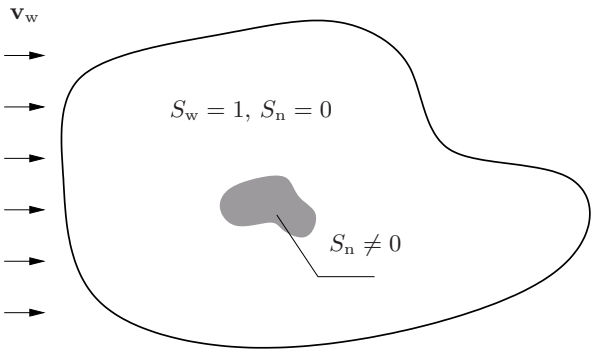

Fig. 9 Multi-physics problem example taken from [60]

5.1.2 Model coupling

Consider a spatial integration of equation (55) as is done for most numerical discretisation. Then the unit of the terms is easily discovered to be volume over time. This basically reveals the phyiscal aspect of the equation, namely the conservation of total fluid volume as also described in Section 3.3.2. The same consideration holds for equation (75), which makes sense since it is derived from the compositional pressure equation. The associated transport equations also have a common physical relevance: the conservation of mass.

The clear relation of the multi-phase compositional and single phase transport model and the possibility to use the same primary variables (as indicated in equation (73)) open the way to couple both models. This makes it possible to fit the model to the actual problem and use a sophisticated and accurate model in a subdomain of special interest, whereas a simpler model can be used in the rest of the domain. Consider for example a large hydrosystem which is fully saturated with water except at a spill of non aqueous phase liquid (NAPL) as displayed in Figure 9. The components of the NAPL are solvable in water and contaminate it. To model the dissolution of the components in the water, only a small area around the NAPL spill has to be discretized by a compositional two-phase model. The spreading of the contaminants in the larger part of the domain can in contrary be simulated using a single-phase transport model. The advantage in coupling the two models in this domain is that in large parts, the costly equilibrium calculations and evaluation of volume derivatives can be avoided.

5.1.3 Practical implementation

The practical implementation of the multi-physics scheme proposed in the preceding sections is done by exploiting the similarity of the equations. Since both pressure equations have the same dimensions and the same unknowns, both can be written into one system of equations. The entries in the stiffnes matrix and right hand side vector are evaluated using either equation (55) if the control volume is situated inside the subdomain or the equation (75) in the other parts of the domain. Equation (55) can also be set up properly at the internal boundary of the subdomain, since all coefficients can be determined. The coefficients concerning the phase which is not present outside the subdomain just have to be set to zero for the outer elements which makes all terms concerning this phase vanish at the boundary. Also the transport equation is well defined at the boundary. Since only one phase is present outside the subdomain, the mobility coefficient in equation (34) will equal zero for all other phases and the multi-phase compositional mass balance will boil down to equation (73) at the interface.

Implicitly, the coupling conditions are already contained in the presented scheme: first, mass fluxes have to be continuous across the subdomain boundary and second, phase velocities have to be continuous across the subdomain boundary. Since only one phase is present outside the subdomain, it is obvious that the second condition requires that only this one phase may flow across the subdomain boundary. Another effect that has to be considered is demixing. Solubilities usually depend on pressure. If a phase is fully saturated with a certain component and then moves further downstream, where the pressure is lower, the solubility decreases and demixing occurs. If the solubility is exceded outside the subdomain this effect is not represented. These two considerations show the crucial importance of an adequate choice of the subdomain. On the one hand, we want the subdomain to be as small as

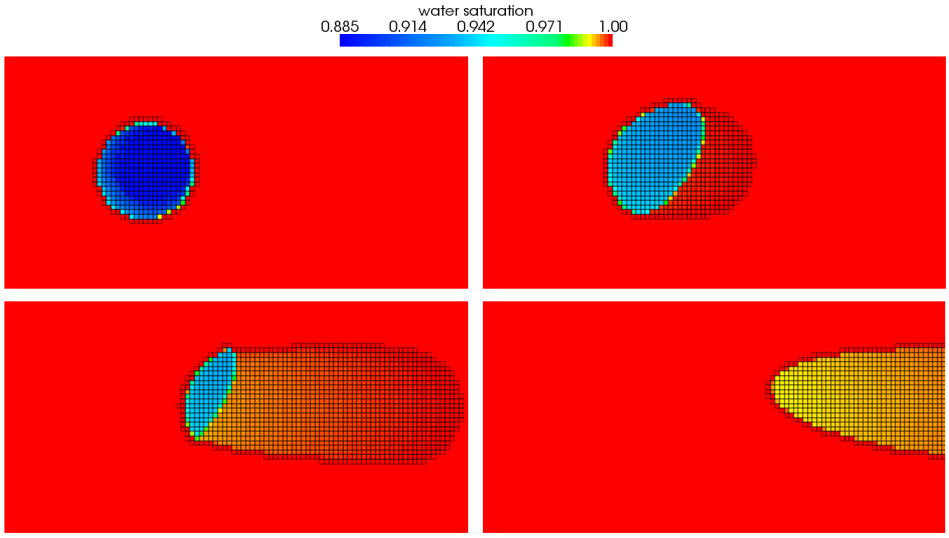

Fig. 10 Dissolution of residual air in water. In black squares: adaptive subdomain at initial conditions, after 100, 200 and 300 timesteps, respectively. taken from [60]

possible to obtain an economic model, on the other hand, it must be chosen large enough to prevent errors. Especially in large and heterogeneous simulation problems, it is unlikely to determine a proper subdomain in advance, so an automatic adaption is sought. As the most logical scheme, we propose to choose all cells with more than one phase and – since demixing occurs predominantly here – all directly adjacent cells to be part of the subdomain. At the end of each timestep, the choice is checked and superfluous cells are removed and necessary cells are added. This quite easy decomposition can only be expected to be successful in the case of an explicit solution of the transport equations. In particular, the fulfilment of the CFL-condition guarantees that no modeling error will occur, since information is transported at most one cell further in one timestep.

As example for the described subdomain adaptivity see Figure 10. Displayed is nearly residual air that moves slightly upward before it is dissolved in water. The subdomain is marked by black squares. In the upper row, the initial subdomain and its expansion due to demixing after 100 timesteps can be seen. In the lower row, one can actually see that cells also get removed from the subdomain and that it moves and finally vanishes with the air phase.

5.1.4 Application example

To demonstrate the performance of the multi-physics approach and to compare it to the full compositional two-phase model on a real life problem, we chose a benchmark problem from carbon-dioxide sequestration as presented in [54] and [35]. Carbon dioxide is injected at a depth of 2960 to 3010 meter into a saline aquifer over a time period of 25 years. The given spatial discretisation consists of 54756 control volumes. Figure 11 shows the results of the simulation runs after 25 years. The result of the multi-physics model on the upper right is obviously in good agreement with the full compositional model. The lower middle displays the subdomain which covers some 4.5 % of the model domain in the last timestep. Using the multi-physics model, the number of calls of the flash calculation could be reduced by a factor of 46 as compared to the full compositional model.

5.2 A multi-scale multi-physics example

We present the multi-scale multi-physics algorithm developed by [100–102] which couples two different physical models:

- a three-phase–three-component model (fine scale, small subdomain)
- a two-phase model (coarse scale, whole domain).

In the following, we present the fine-scale equation system for describing these processes.

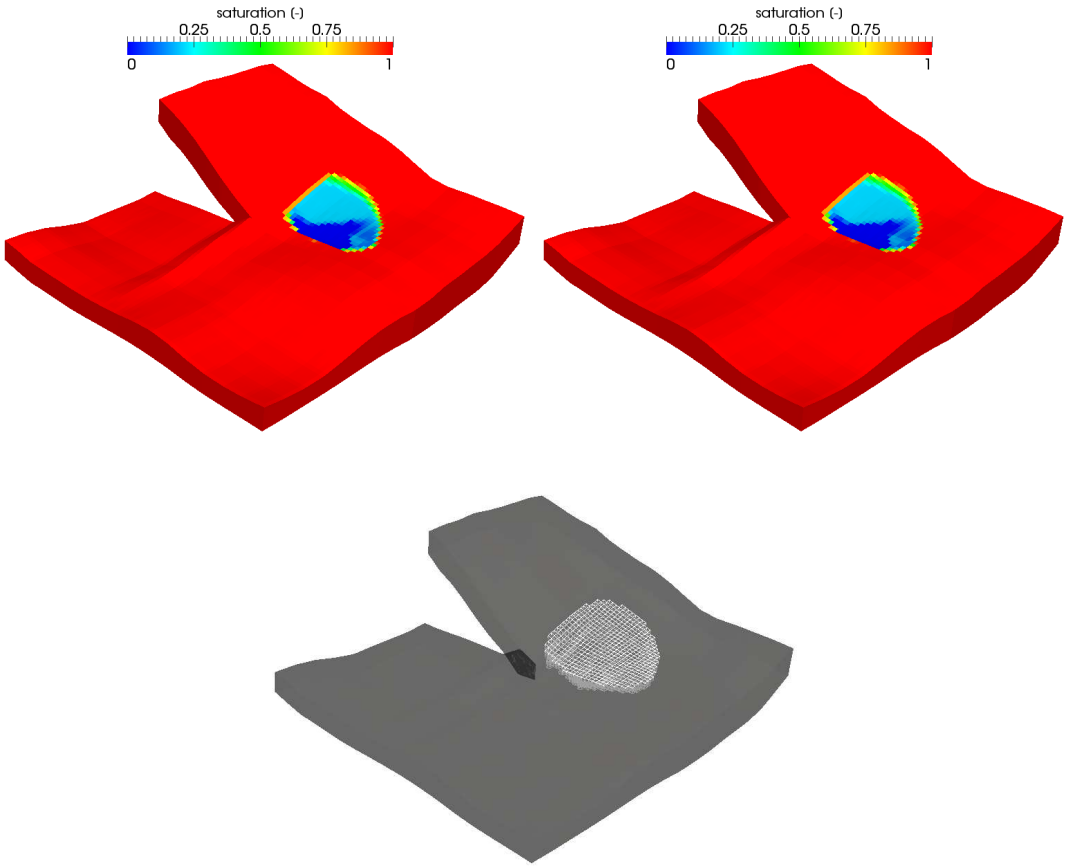

Fig. 11 Results for the Johannsen formation benchmark after 25 years. Upper left: full compositional two-phase model, upper right: multi-physics approach, lower middle: subdomain of multi-physics approach

Three-phase three-component model The three considered phases are the wetting phase w (might be water), an intermediate-wetting phase n (might be an oil), and a non-wetting phase g (which could be a gas). Neglecting gravitational and capillary forces (which are not negligible in many physical systems, of course, but we do so in order to set up the algorithm) and assuming constant densities and viscosities, three-phase three component flow and transport can be described by a pressure equation and two concentration equations in the following way.

The pressure equation is given as

$$\nabla \cdot (\lambda_{\mathrm{t}} \mathbf{K} \nabla p) = 0. \tag{76}$$

Using extended Darcy's law, the Darcy velocity $\mathbf{v}_{\mathrm{t}}$ can be reconstructed as $\mathbf{v}_{\mathrm{t}} = -\lambda_{\mathrm{t}} \mathbf{K} \nabla p$.

The concentration equations yield

$$\frac{\partial C^{\kappa}}{\partial t} + \mathbf{v}_{\mathrm{t}} \cdot \nabla \sum_{\alpha} (f_{\alpha} \varrho_{\alpha} X_{\alpha}^{\kappa}) = 0 \qquad \kappa \in \{1, 2\}. \tag{77}$$

Note that source and sink terms have been skipped for simplicity. Given the total concentrations and the pressure, saturations can be calculated using flash calculation (see section 4.2.2).

Two-phase model We consider a porous medium occupied by a wetting-phase w and a non-wetting gas phase g. The flow of the two phases is described by the pressure equation as given in equation (76) with the only difference that λ_{t} is fully defined by knowing one of the saturations, $\lambda_{\mathrm{t}} = \lambda_{\mathrm{t}}(S_{\mathrm{w}})$.

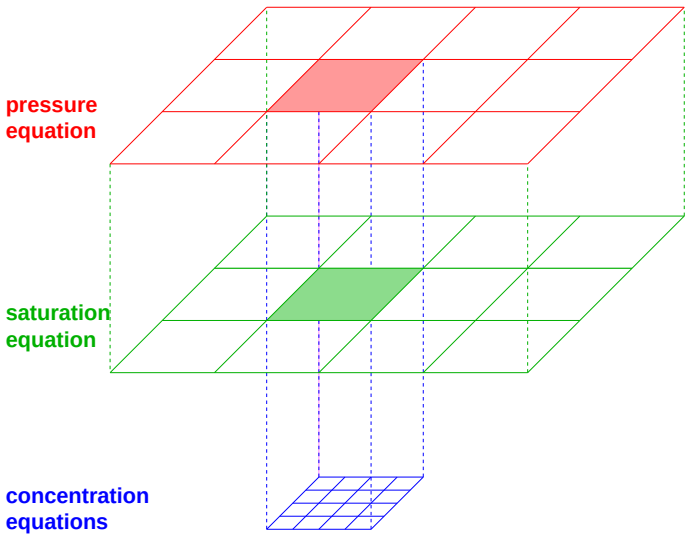

Fig. 12 Scales and solution domain for pressure, saturation, and concentration equations in the multi-scale multi-physcis algorithm.

The second equation needed is the saturation equation,

$$\frac{\partial S_{\mathrm{w}}}{\partial t} + \mathbf{v}_{\mathrm{t}} \cdot \nabla f_{\mathrm{w}} = 0, \tag{78}$$

where again, source / sink terms are skipped for sake of simplicity.

5.2.1 Multi-scale multi-physics algorithm

Figure 12 shows on which scales and in which parts of the domain which equation is solved: pressure and saturation equation are solved in the whole domain and on the coarse scale, while the concentration equations are only solved in a subdomain of interest and on the fine scale. The corresponding multi-scale multi-physics algorithm is presented in the context of a discontinuous Galerkin finite element discretization of the partial differential equations using the method given by [15] as this scheme is used for calculating the numerical results. However, after slight modifications of the algorithm, other discretization schemes are possible. The elliptic pressure equation is solved using an time-implicit Runge-Kutta scheme. The linear equation system arising from the implicit Runge-Kutta time stepping is preconditioned with a smoother and solved using a linear multi-grid solver. Hyperbolic / parabolic saturation and concentration equations are solved time-explicitly using an S-stable 3-stage Runge-Kutta method of order 3 with a modified minmod flux limiter as given in [38]. The overall algorithm consists of the following steps.

1. Calculate coarse-scale intrinsic permeabilities.
2. Solve the coarse-scale pressure equation in the total domain.
3. Calculate the coarse-scale velocity field and make it continuous across coarse-element edges.
4. Calculate fine-scale velocities in the subdomain using downscaling and make them continuous across fine-element edges.
5. Solve two concentration equations in the subdomain using Dirichlet boundary conditions and n micro time steps. The latter is necessary in order to fulfill the Courant-Friedrich-Lewy stability criterion for the explicitly solved concentration equations. Here, n is the ratio of coarse-grid discretization length over fine-grid discretization length. Note that the boundary conditions may vary with time as total concentrations depend on saturation.
6. Calculate fine-scale saturations in the subdomain using flash calculations and average them over coarse-scale elements.
7. Solve the coarse-scale saturation equation using these averaged saturations in the subdomain and a source / sink term that makes up for possible mass losses / gains due to changing saturations in the subdomain.

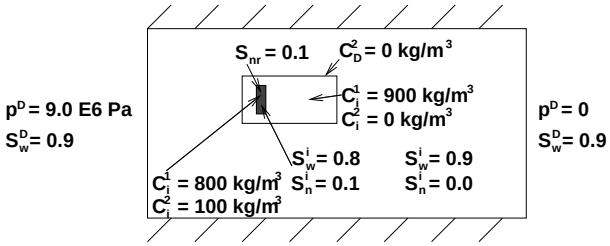

Fig. 13 Setup of example 2. Boundary and initial conditions as well as size and location of the subdomain and the residual LNAPL contamination are shown.

Fig. 14 Water saturation contours for three different test cases. Left hand side: fine-scale reference solution, middle: saturation equation is upscaled and pressure equation is solved on the fine scale, right hand side: both pressure and saturation equation are upscaled.

8. Use new saturation field and go to step 2.

Step (7) is necessary as averaged saturations obtained through flash calculations from the solution of local fine-scale concentration equations generally differ from saturations obtained from solving the upscaled saturation equation. This is because in the first case, two-phase two-component processes are accounted for while in the second case, only a two-phase problem is solved. As two-phase two-component processes are the governing processes within the subdomain, these saturations are assumed to be correct and plugged into the solution of the upscaled saturation equation. Now, in order to maintain local mass conservation, a source / sink term within each coarse-scale element is needed that makes up for this difference in mass.

5.2.2 Numerical results

We consider a domain with a geostatistically generated intrinsic permeability field given on the fine scale. Pressure, saturation, and concentration equations are solved (i.e. mass transfer is taking place in a subdomain) as shown in Figure 12. Figure 13 shows the boundary and initial conditions as well as the spatial extension of the subdomain where mass transfer is accounted for by solving concentration equations and using flash calculations to distribute components among phases. In a part of the subdomain, there is a residual LNAPL contamination of an initial saturation of $S_n = 0.1$. Again, there is a pressure gradient from left to right and top as well as bottom boundary are closed. Wetting-phase saturation is equal to 0.9 everywhere except for a small part of the subdomain where mass transfer is accounted for (here, wetting-phase saturation is 0.1). Finally, Dirichlet boundary conditions for total concentrations are given such that water and gas phase on the boundary of the subdomain are consisting of water component only, respectively air component only. The motivation for that choice of boundary conditions at the subdomain boundary is that this subdomain has to be chosen sufficiently large in order to capture the whole region where mass transfer is taking place. The residual LNAPL initially consists of LNAPL component only. While three-phase water–LNAPL–gas relative permeability–saturation relationships after [129] in combination with [107] are used in the subdomain, in the remaining part of the domain, two-phase Van Genuchten functions are chosen.

Figure 14 compares water saturation contours at a certain point of time (after 59 hours) using the extended multi-scale multi-physics algorithm (both pressure and saturation equation are upscaled), the original multi-scale multi-physics algorithm (only the saturation equation is upscaled), and the fine-scale reference solution. The location of the subdomain where three-phase–three-component processes are modeled corresponds to the region within the white rectangle. It can be seen that water saturation

changes downstream of the residual LNAPL plume and also within the region where the LNAPL is present. As the LNAPL cannot move the change of water saturation must be due to mass transfer processes. Neither the model where the saturation equation is upscaled nor the model where both saturation and pressure equation are upscaled can capture all the details of the fine-scale reference solution. But still, the principal features of the saturation distribution can be captured. Also, the agreement between the results using saturation upscaling only and the results using the model with upscaled pressure and saturation equation is excellent. This indicates again that pressure upscaling and velocity downscaling preserves a high accuracy of the fine-scale velocity field.

6 Conclusion

In this work, we have given an overview of multi-scale multi-physics methods for flow and transport processes in porous media. Therefore, we defined relevant scales and gave an overview of multi-scale and of multi-physics methods. We introduced the mathematical model for compositional non-isothermal multi-phase flow and transport in porous media and discussed possible mathematical formulations. Based on that, decoupled and coupled numerical solution strategies are discussed. In a next part, applications examples of multi-physics and of multi-scale multi-physics models were given. This work is meant to give an overview of existing multi-scale multi-physics approaches for multi-phase flow problems in porous media. Examples are given in order to illustrate the effectiveness and applicability of these algorithms.

Future work needs to be done to include more complex processes in the multi-scale multi-physics algorithms in order to allow for the modeling of highly complex real-life systems. Also, the development of upscaling techniques and the upscaling of the complex equations is a crucial issue. Coupling techniques need to be improved to allow for a physically based coupling of different multi-physics domains and for the coupling across scales. Numerical methods need to be improved in order to allow for moving meshes if the multi-physics domains move during a simulation and multi-scale multi-physics algorithms need to allow for the application of different numerical schemes for the solution of different physical processes (multi-numerics).

In conclusion, we state that the development and application of multi-scale multi-physics techniques allows to model highly complex physical problems in large domains that could otherwise not be solved numerically.

References

1. Aarnes, J. E., Krogstad, S., and Lie, K.-A. (2006). A hierarchical multiscale method for two-phase flow based upon mixed finite elements and nonuniform coarse grids. *Multiscale Model. Simul.*, 5(2):337–363.
2. Aarnes, J. E., Krogstad, S., and Lie, K.-A. (2008). Multiscale mixed/mimetic methods on corner-point grids. *Comput. Geosci.*, 12(3):297–315.
3. Aavatsmark, I. (2002). An introduction to multipoint flux approximations for quadrilateral grids. *Comput. Geosci.*, 6(3-4):405–432. Locally conservative numerical methods for flow in porous media.
4. Aavatsmark, I., Eigestad, G. T., Mallison, B. T., and Nordbotten, J. M. (2008). A compact multipoint flux approximation method with improved robustness. *Numer. Methods Partial Differential Equations*, 24(5):1329–1360.
5. Ainsworth, M. and Oden, J. T. (2000). *A posteriori error estimation in finite element analysis*. Pure and Applied Mathematics (New York). Wiley-Interscience [John Wiley & Sons], New York.
6. Albon, C., Jaffre, J., Roberts, J., Wang, X., and Serres, C. (1999). Domain decompositioning for some transition problems in flow in porous media. In Chen, Z., Ewing, R., and Shi, Z.-C., editors, *Numerical Treatment of Multiphase Flow in Porous Media*, Lecture Notes in Physics. Springer.
7. Allen, M. B., Ewing, R. E., and Lu, P. (1992). Well-conditioned iterative schemes for mixed finite-element models of porous-media flows. *SIAM J. Sci. Statist. Comput.*, 13(3):794–814.
8. Arbogast, T. (1989). Analysis of the simulation of single phase flow through a naturally fractured reservoir. *SIAM J. Numer. Anal.*, 26(1):12–29.
9. Arbogast, T., Pencheva, G., Wheeler, M. F., and Yotov, I. (2007). A multiscale mortar mixed finite element method. *Multiscale Model. Simul.*, 6(1):319–346.

10. Atkins, P. (1994). *Physical Chemsitry*. Oxford University Press, fifth edition edition.
11. Aziz, K. and Settari, A. (1979). *Petroleum Reservoir Simulation*. Elsevier Applied Science.
12. Aziz, K. and Wong, T. (1989). Considerations in the development of multipurpose reservoir simulation models. In *Proceedings First and Second International Forum on Reservoir Simulation*, pages 77–208. Steiner, P.
13. Babuska, I. and Strouboulis, T. (2001). *The finite element method and its reliability*. Numerical Mathematics and Scientific Computation. The Clarendon Press Oxford University Press, New York.
14. Barker, J. and Thibeau, S. (1997). A critical review of the use of pseudorelative permeabilities for upscaling. *SPE Reservoir Engineering*, 12(2):138–143.
15. Bastian, P. (2003). Higher Order Discontinuous Galerkin Methods for Flow and Transport in Porous Media. In Bänsch, E., editor, *Challenges in Scientific Computing – CISC 2002*, number 35 in LNCSE.
16. Bastian, P. and Rivière, B. (2003). Superconvergence and $H(\mathrm{div})$ projection for discontinuous Galerkin methods. *Internat. J. Numer. Methods Fluids*, 42(10):1043–1057.
17. Beavers, G. S. and Joseph, D. D. (1967). Boundary conditions at a naturally permeable wall. *J. Fluid Mech.*, 30:197–207.
18. Berndt, M., Lipnikov, K., Shashkov, M., Wheeler, M. F., and Yotov, I. (2005). Superconvergence of the velocity in mimetic finite difference methods on quadrilaterals. *SIAM J. Numer. Anal.*, 43(4):1728–1749.
19. Binning, P. and Celia, M. A. (1999). Practical implementation of the fractional flow approach to multi-phase flow simulation. *Advances in Water Resources*, 22(5):461–478.
20. Bramble, J. H. (1993). *Multigrid methods*, volume 294 of *Pitman Research Notes in Mathematics Series*. Longman Scientific & Technical, Harlow.
21. Brezzi, F. and Fortin, M. (1991). *Mixed and hybrid finite element methods*, volume 15 of *Springer Series in Computational Mathematics*. Springer-Verlag, New York.
22. Brezzi, F., Lipnikov, K., and Shashkov, M. (2005a). Convergence of the mimetic finite difference method for diffusion problems on polyhedral meshes. *SIAM J. Numer. Anal.*, 43(5):1872–1896.
23. Brezzi, F., Lipnikov, K., and Simoncini, V. (2005b). A family of mimetic finite difference methods on polygonal and polyhedral meshes. *Math. Models Methods Appl. Sci.*, 15(10):1533–1551.
24. Briggs, W. L., Henson, V. E., and McCormick, S. F. (2000). *A multigrid tutorial*. Society for Industrial and Applied Mathematics (SIAM), Philadelphia, PA, second edition.
25. Cao, Y., Helmig, R., and Wohlmuth, B. (2008). The influence of the boundary discretization on the multipoint flux approximation L-method. In *Finite volumes for complex applications V*, pages 257–263. ISTE, London.
26. Cattani, C. and Laserra, E. (2003). Wavelets in the transport theory of heterogeneous reacting solutes. *Int. J. Fluid Mech. Res.*, 30(2):147–152.
27. Chavent, G. (1976). *A new formulation of diphasic incompressible flows in porous media*, pages 258–270. Number 503 in Lecture Notes in Mechanics. Springer, Berlin.
28. Chavent, G. and Jaffré, J. (1986). *Mathematical models and finite elements for reservoir simulation*. North-Holland, Amsterdam.
29. Chen, Y. and Durlofsky, L. J. (2006). Adaptive local-global upscaling for general flow scenarios in heterogeneous formations. *Transport in Porous Media*, 62(2):157–185.
30. Chen, Y., Durlofsky, L. J., Gerritsen, M., and Wen, X. H. (2003). A coupled local-global upscaling approach for simulating flow in highly heterogeneous formations. *Advances in Water Resources*, 26(10):1041–1060.
31. Chen, Z., Ewing, R. E., Jiang, Q., and Spagnuolo, A. M. (2002). Degenerate two-phase incompressible flow. V. Characteristic finite element methods. *J. Numer. Math.*, 10(2):87–107.
32. Chen, Z., Guan, Q., and Ewing, R. (2000). Analysis of a compositional model for fluid flow in porous media. *SIAM Journal on Applied Mathematics*, 60(3):747–777.
33. Chen, Z. and Hou, T. Y. (2002). A mixed multiscale finite element method for elliptic problems with oscillating coefficients. *Mathematics of Computation*, 72(242):541–576.
34. Chen, Z., Huan, G., and Ma, Y. (2006). *Computational Methods for Multiphase Flows in Porous Media*. SIAM, Computational Science & Engineering.
35. Class, H., Ebigbo, A., Helmig, R., Dahle, H., Nordbotten, J., Celia, M., Audigane, P., Darcis, M., Ennis-King, J., Fan, Y., Flemisch, B., Gasda, S., Jin, M., Krug, S., Labregere, D., Naderi Beni, A., Pawar, R., Sbai, A., Thomas, S., Trenty, L., and Wei, L. (in press, DOI:10.1007/s10596-009-9146-

x). A benchmark study on problems related to co2 storage in geologic formations: Summary and discussion of the results. *Computational Geosciences*.
36. Cockburn, B., Lin, S. Y., and Shu, C.-W. (1989). TVB Runge-Kutta local projection discontinuous Galerkin finite element method for conservation laws. III. One-dimensional systems. *J. Comput. Phys.*, 84(1):90–113.
37. Cockburn, B. and Shu, C.-W. (1989). TVB Runge-Kutta local projection discontinuous Galerkin finite element method for conservation laws. II. General framework. *Math. Comp.*, 52(186):411–435.
38. Cockburn, B. and Shu, C.-W. (1998). The Runge-Kutta Discontinuous Galerkin Method for Conservation laws V: Multidimensional Systems. *Journal of Computational Physics*, 141:199–224.
39. Codina, R. (2001). A stabilized finite element method for generalized stationary incompressible flows. *Comput. Methods Appl. Mech. Engrg.*, 190(20-21):2681–2706.
40. Darman, N. H., Pickup, G. E., and Sorbie, K. S. (2002). A comparison of two-phase dynamic upscaling methods based on fluid potentials. *Computational Geosciences*, 6(1):5–27.
41. Dawson, C. N., Russell, T. F., and Wheeler, M. F. (1989). Some improved error estimates for the modified method of characteristics. *SIAM J. Numer. Anal.*, 26(6):1487–1512.
42. Dennis, Jr., J. E. and Schnabel, R. B. (1996). *Numerical methods for unconstrained optimization and nonlinear equations*, volume 16 of *Classics in Applied Mathematics*. Society for Industrial and Applied Mathematics (SIAM), Philadelphia, PA.
43. Dietrich, P., Hemlig, R., Sauter, M., Hötzl, H., Köngeter, J., and Teutsch, G., editors (2005). *Flow and Transport in Fractured Porous Media*. Springer.
44. Discacciati, M., Miglio, E., and A., Q. (2002). Mathematical and numerical models for coupling surface and groundwater flows. *Appl. Num. Math.*, 43:57–74.
45. Douglas, Jr., J., Huang, C.-S., and Pereira, F. (1999). The modified method of characteristics with adjusted advection. *Numer. Math.*, 83(3):353–369.
46. Durlofsky, L. J. (1991). Numerical Calculation of Equivalent Grid Block Permeability Tensors for Heterogeneous Porous Media. *Water Resources Research*, 27(5):699–708.
47. E, W. and Engquist, B. (2003a). The heterogeneous multiscale methods. *Commun. Math. Sci.*, 1(1):87–132.
48. E, W. and Engquist, B. (2003b). Multiscale modeling and computation. *Notices Amer. Math. Soc.*, 50(9):1062–1070.
49. E, W., Engquist, B., and Huang, Z. (2003). Heterogeneous multiscale method: A general methodology for multiscale modeling . *Physical Review*, 67.
50. E, W., Engquist, B., Li, X., Ren, W., and Vanden-Eijnden, E. (2007). Heterogeneous multiscale methods: a review. *Commun. Comput. Phys.*, 2(3):367–450.
51. Efendiev, Y. and Durlofsky, L. J. (2002). Numerical modeling of subgrid heterogeneity in two phase flow simulations. *Water Resources Research*, 38(8).
52. Efendiev, Y., Durlofsky, L. J., and Lee, S. H. (2000). Modeling of subgrid effects in coarse-scale simulations of transport in heterogeneous porous media. *Water Resources Research*, 36(8):2031 – 2041.
53. Efendiev, Y. and Hou, T. (2007). Multiscale finite element methods for porous media flows and their applications. *Appl. Numer. Math.*, 57(5-7):577–596.
54. Eigestad, G., Dahle, H., Hellevang, B., Johansen, W., Riis, F., and Øian, E. (in press, DOI:10.1007/s10596-009-9153-y). Geological modeling and simulation of co2 injection in the johansen formation. *Computational Geosciences*.
55. Eigestad, G. T. and Klausen, R. A. (2005). On the convergence of the multi-point flux approximation O-method: numerical experiments for discontinuous permeability. *Numer. Methods Partial Differential Equations*, 21(6):1079–1098.
56. Ewing, R. E., Russell, T. F., and Wheeler, M. F. (1984). Convergence analysis of an approximation of miscible displacement in porous media by mixed finite elements and a modified method of characteristics. *Comput. Methods Appl. Mech. Engrg.*, 47(1-2):73–92.
57. Ewing, R. E. and Wang, H. (1994). Eulerian-Lagrangian localized adjoint methods for variable-coefficient advective-diffusive-reactive equations in groundwater contaminant transport. In *Advances in optimization and numerical analysis (Oaxaca, 1992)*, volume 275 of *Math. Appl.*, pages 185–205. Kluwer Acad. Publ., Dordrecht.
58. Ewing, R. E. and Wang, H. (1996). An optimal-order estimate for Eulerian-Lagrangian localized adjoint methods for variable-coefficient advection-reaction problems. *SIAM J. Numer. Anal.*,

33(1):318–348.
59. Eymard, R., Gallouët, T., and Herbin, R. (2000). Finite volume methods. In *Handbook of numerical analysis, Vol. VII*, Handb. Numer. Anal., VII, pages 713–1020. North-Holland, Amsterdam.
60. Fritz, J., Flemisch, B., and Helmig, R. (submitted, preprint on www.nupus.uni-stuttgart.de number 2009/8). Multiphysics modeling of advection-dominated two-phase compositional flow in porous media. *International Journal of Numerical Analysis & Modeling*.
61. Ghostine, R., Kesserwani, G., Mosé, R., Vazquez, J., and Ghenaim, A. (2009). An improvement of classical slope limiters for high-order discontinuous Galerkin method. *Internat. J. Numer. Methods Fluids*, 59(4):423–442.
62. Giraud, L., Langou, J., and Sylvand, G. (2006). On the parallel solution of large industrial wave propagation problems. *J. Comput. Acoust.*, 14(1):83–111.
63. Girault, V. and Rivière, B. (2009). Dg approximation of coupled navier-stokes and darcy equations by beaver-joseph-saffman interface condition. *SIAM J. Numer. Anal.*, 47:2052–2089.
64. Gray, G. W., Leijnse, A., Kolar, R. L., and Blain, C. A. (1993). *Mathematical Tools for Changing Scale in the Analysis of Physical Systems*. CRC, 1 edition.
65. Hajibeygi, H., Bonfigli, G., Hesse, M. A., and Jenny, P. (2008). Iterative multiscale finite-volume method. *J. Comput. Phys.*, 227(19):8604–8621.
66. Hauke, G. and García-Olivares, A. (2001). Variational subgrid scale formulations for the advection-diffusion-reaction equation. *Comput. Methods Appl. Mech. Engrg.*, 190(51-52):6847–6865.
67. He, Y. and Han, B. (2008). A wavelet finite-difference method for numerical simulation of wave propagation in fluid-saturated porous media. *Appl. Math. Mech. (English Ed.)*, 29(11):1495–1504.
68. Helmig, R. (1997). *Multiphase Flow and Transport Processes in the Subsurface*. Springer.
69. Herrera, I., Ewing, R. E., Celia, M. A., and Russell, T. F. (1993). Eulerian-Lagrangian localized adjoint method: the theoretical framework. *Numer. Methods Partial Differential Equations*, 9(4):431–457.
70. Hoteit, H., Ackerer, P., Mosé, R., Erhel, J., and Philippe, B. (2004). New two-dimensional slope limiters for discontinuous Galerkin methods on arbitrary meshes. *Internat. J. Numer. Methods Engrg.*, 61(14):2566–2593.
71. Hoteit, H. and Firoozabadi, A. (2008). Numerical modeling of two-phase flow in heterogeneous permeable media with different capillarity pressures. *Advances in Water Resources*, 31(1):56–73.
72. Hou, T. Y. and Wu, X.-H. (1997). A multiscale finite element method for elliptic problems in composite materials and porous media. *J. Comput. Phys.*, 134(1):169–189.
73. Hristopulos, D. and G.Christakos (1997). An analysis of hydraulic conductivity upscaling. *Nonlinear Analysis*, 30(8):4979–4984.
74. Huang, C.-S. (2000). Convergence analysis of a mass-conserving approximation of immiscible displacement in porous media by mixed finite elements and a modified method of characteristics with adjusted advection. *Comput. Geosci.*, 4(2):165–184.
75. Hughes, T. J. R. (1995). Multiscale phenomena: Green's functions, the Dirichlet-to-Neumann formulation, subgrid scale models, bubbles and the origins of stabilized methods. *Comput. Methods Appl. Mech. Engrg.*, 127(1-4):387–401.
76. Hughes, T. J. R., Feijóo, G. R., Mazzei, L., and Quincy, J.-B. (1998). The variational multiscale method—a paradigm for computational mechanics. *Comput. Methods Appl. Mech. Engrg.*, 166(1-2):3–24.
77. Hyman, J., Morel, J., Shashkov, M., and Steinberg, S. (2002). Mimetic finite difference methods for diffusion equations. *Comput. Geosci.*, 6(3-4):333–352. Locally conservative numerical methods for flow in porous media.
78. IPCC (2005). *Carbon Dioxide Capture and Storage. Special Report of the Intergovernmental Panel on Climate Change*. Cambridge University Press.
79. Jäger, W. and Mikelić, A. (2009). Modeling effective interface laws for transport phenomena between an unconfined fluid and a porous medium using homogenization. *Transp. Porous Media*, 78:489–508.
80. Jang, G.-W., Kim, J. E., and Kim, Y. Y. (2004). Multiscale Galerkin method using interpolation wavelets for two-dimensional elliptic problems in general domains. *Internat. J. Numer. Methods Engrg.*, 59(2):225–253.
81. Jenny, P., Lee, S. H., and Tchelepi, H. (2003). Multi-scale finite-volume method for elliptic problems in subsurface flow simulations. *Journal of Computational Physics*, 187:47–67.

82. Jenny, P., Lee, S. H., and Tchelepi, H. A. (2006). Adaptive fully implicit multi-scale finite-volume method for multi-phase flow and transport in heterogeneous porous media. *J. Comput. Phys.*, 217(2):627–641.
83. Juanes, R. (2005). A variational multiscale finite element method for multiphase flow in porous media. *Finite Elem. Anal. Des.*, 41(7-8):763–777.
84. Juanes, R. and Lie, K.-A. (2008). Numerical modeling of multiphase first-contact miscible flows. II. Front-tracking/streamline simulation. *Transp. Porous Media*, 72(1):97–120.
85. Kim, M.-Y., Park, E.-J., Thomas, S. G., and Wheeler, M. F. (2007). A multiscale mortar mixed finite element method for slightly compressible flows in porous media. *J. Korean Math. Soc.*, 44(5):1103–1119.
86. Kippe, V., Aarnes, J. E., and Lie, K.-A. (2008). A comparison of multiscale methods for elliptic problems in porous media flow. *Comput. Geosci.*, 12(3):377–398.
87. Klausen, R. A. and Winther, R. (2006). Robust convergence of multi point flux approximation on rough grids. *Numer. Math.*, 104(3):317–337.
88. Layton, W. J., Schieweck, F., and Yotov, I. (2003). Coupling fluid flow with porous media flow. *SIAM J. Numer. Anal.*, 40:2195–2218.
89. Lee, S. H., Wolfsteiner, C., and Tchelepi, H. A. (2008). Multiscale finite-volume formulation of multiphase flow in porous media: black oil formulation of compressible, three-phase flow with gravity. *Comput. Geosci.*, 12(3):351–366.
90. LeVeque, R. J. (2002). *Finite volume methods for hyperbolic problems*. Cambridge Texts in Applied Mathematics. Cambridge University Press, Cambridge.
91. Lüdecke, C. and Lüdecke, D. (2000). *Thermodynamik*. Springer, Berlin.
92. Lunati, I. and Jenny, P. (2006). Multiscale finite-volume method for compressible multiphase flow in porous media. *J. Comput. Phys.*, 216(2):616–636.
93. Lunati, I. and Jenny, P. (2007). Treating highly anisotropic subsurface flow with the multiscale finite-volume method. *Multiscale Model. Simul.*, 6(1):308–318.
94. Lunati, I. and Jenny, P. (2008). Multiscale finite-volume method for density-driven flow in porous media. *Comput. Geosci.*, 12(3):337–350.
95. Matringe, S. F., Juanes, R., and Tchelepi, H. A. (2006). Robust streamline tracing for the simulation of porous media flow on general triangular and quadrilateral grids. *J. Comput. Phys.*, 219(2):992–1012.
96. Mazzia, A. and Putti, M. (2006). Three-dimensional mixed finite element-finite volume approach for the solution of density-dependent flow in porous media. *J. Comput. Appl. Math.*, 185(2):347–359.
97. Michelsen, M. and Mollerup, J. (2007). *Thermodynamic Models: Fundamentals & Computational Aspects*. Tie-Line Publications, Denmark.
98. Müller, S. (2003). *Adaptive multiscale schemes for conservation laws*, volume 27 of *Lecture Notes in Computational Science and Engineering*. Springer-Verlag, Berlin.
99. Nghiem, L. and Li, Y.-K. (1984). Computation of multiphase equilibrium phenomena with an equation of state. *Fluid Phase Equilibria*, 17(1):77–95.
100. Niessner, J. and Helmig, R. (2006). Multi-scale modeling of two-phase - two-component processes in heterogeneous porous media. *Numerical Linear Algebra with Applications*, 13(9):699–715.
101. Niessner, J. and Helmig, R. (2007). Multi-scale modeling of three-phase–three-component processes in heterogeneous porous media. *Advances in Water Resources*, 30(11):2309–2325.
102. Niessner, J. and Helmig, R. (2009). Multi-physics modeling of flow and transport in porous media using a downscaling approach. *Advances in Water Resources*, 32(6):845–850.
103. Nordbotten, J. M. and Bjørstad, P. E. (2008). On the relationship between the multiscale finite-volume method and domain decomposition preconditioners. *Comput. Geosci.*, 12(3):367–376.
104. Of, G. (2007). Fast multipole methods and applications. In *Boundary element analysis*, volume 29 of *Lect. Notes Appl. Comput. Mech.*, pages 135–160. Springer, Berlin.
105. Oladyshkin, S., Royer, J.-J., and Panfilov, M. (2008). Effective solution through the streamline technique and HT-splitting for the 3D dynamic analysis of the compositional flows in oil reservoirs. *Transp. Porous Media*, 74(3):311–329.
106. Panfilov, M. (2000). *Macroscale models of flow through highly heterogeneous porous media*. Kluwer Academic Publishers.
107. Parker, J. C., Lenhard, R. J., and Kuppusami, T. (1987). A Parametric Model for Constitutive Properties Governing Multiphase Flow in Porous Media. *Water Resources Research*, 23(4):618–624.

108. Peszynska, M., Lu, Q., and Wheeler, M. (2000). Multiphysics coupling of codes. In *Computational Methods in Water Resources*, pages 175–182. A. A. Balkema.
109. Peszynska, M., Wheeler, M. F., and Yotov, I. (2002). Mortar upscaling for multiphase flow in porous media. *Computational Geosciences*, 6:73–100.
110. Prausnitz, J. M., Lichtenthaler, R. N., and Azevedo, E. G. (1967). *Molecular Thermodynamics of Fluid-Phase Equilibria*. Prentice-Hall.
111. Pruess, K. (1985). A practical method for modeling fluid and heat flow in fractured porous media. *SPE Journal*, 25(1):14–26.
112. Renard, P. and de Marsily, G. (1997). Calculating effective permeability: a review. *Advances in Water Resources*, 20:253 – 278.
113. Russell, T. F. (1990). Eulerian-Lagrangian localized adjoint methods for advection-dominated problems. In *Numerical analysis 1989 (Dundee, 1989)*, volume 228 of *Pitman Res. Notes Math. Ser.*, pages 206–228. Longman Sci. Tech., Harlow.
114. Ryzhik, V. (2007). Spreading of a NAPL lens in a double-porosity medium. *Comput. Geosci.*, 11(1):1–8.
115. Scheidegger, A. (1974). *The physics of flow through porous media*. University of Toronto Press, 3d edition.
116. Shashkov, M. (1996). *Conservative finite-difference methods on general grids*. Symbolic and Numeric Computation Series. CRC Press, Boca Raton, FL.
117. Sheldon, J. W. and Cardwell, W. T. (1959). One-dimensional, incompressible, noncapillary, two-phase fluid in a porous medium. *Petroleum Trans. AIME*, 216:290–296.
118. Sleep, B. E. and Sykes, J. F. (1993). Compositional simulation of groundwater contamination by organic-compounds. 1. model developement and verification. *Water Resources Research*, 29(6):1697–1708.
119. Smith, E. H. and Seth, M. S. (1999). Efficient solution for matrix-fracture flow with multiple interacting continua. *Int. J. Numer. Anal. Methods Geomech.*, 23(5):427–438.
120. Srinivas, C., Ramaswamy, B., and Wheeler, M. F. (1992). Mixed finite element methods for flow through unsaturated porous media. In *Computational methods in water resources, IX, Vol. 1 (Denver, CO, 1992)*, pages 239–246. Comput. Mech., Southampton.
121. Stenby, E. and Wang, P. (1993). Noniterative phase equilibrium calculation in compositional reservoir simulation. *SPE 26641*.
122. Stone, H. L. and Garder Jr., A. O. (1961). Analysis of gas-cap or dissolved-gas reservoirs. *Petroleum Trans. AIME*, 222:92–104.
123. Stüben, K. (2001). A review of algebraic multigrid. *J. Comput. Appl. Math.*, 128(1-2):281–309. Numerical analysis 2000, Vol. VII, Partial differential equations.
124. Suk, H. and Yeh, G.-T. (2008). Multiphase flow modeling with general boundary conditions and automatic phase-configuration changes using a fractional-flow approach. *Computational Geosciences*, 12(4):541–571.
125. Tornberg, A.-K. and Greengard, L. (2008). A fast multipole method for the three-dimensional Stokes equations. *J. Comput. Phys.*, 227(3):1613–1619.
126. Trangenstein, J. and Bell, J. (1989). Mathematical structure of compositional reservoir simulation. *SIAM J. Sci. Stat. Comput.*, 10(5):817–845.
127. Trottenberg, U., Oosterlee, C. W., and Schüller, A. (2001). *Multigrid*. Academic Press Inc., San Diego, CA.
128. Urban, K. (2009). *Wavelet methods for elliptic partial differential equations*. Numerical Mathematics and Scientific Computation. Oxford University Press, Oxford.
129. Van Genuchten, M. T. (1980). A Closed-Form Equation for Predicting the Hydraulic Conductivity of Unsaturated Soils. *American Journal of Soil Science*, 44:892–898.
130. Wallstrom, T. C., Christie, M. A., Durlofsky, L. J., and Sharp, D. H. (2002a). Effective flux boundary conditions for upscaling porous media equations. *Transport in Porous Media*, 46(2):139–153.
131. Wallstrom, T. C., Hou, S., Christie, M. A., Durlofsky, L. J., Sharp, D. H., and Zou, Q. (2002b). Application of effective flux boundary conditions to two-phase upscaling in porous media. *Transport in Porous Media*, 46(2):155–178.
132. Wang, H., Liang, D., Ewing, R. E., Lyons, S. L., and Qin, G. (2002). An ELLAM approximation for highly compressible multicomponent flows in porous media. *Comput. Geosci.*, 6(3-4):227–251.

Locally conservative numerical methods for flow in porous media.
133. Wang, P. and Barker, J. (1995). Comparison of flash calculations in compositional reservoir simulation. *SPE 30787*.
134. Wheeler, M., Arbogast, T., Bryant, S., Eaton, J., Lu, Q., Peszynska, M., and Yotov, I. (1999). A parallel multiblock/multidomain approach to reservoir simulation. In *Fifteenth SPE Symposium on Reservoir Simulation, Houston, Texas*, pages 51–62. Society of Petroleum Engineers. SPE 51884.
135. Whitaker, S. (1998). *The method of volume averaging*. Kluwer Academic Publishers.
136. White, F. (2003). *Fluid Mechanics*. McGraw-Hill.
137. Yao, Z.-H., Wang, H.-T., Wang, P.-B., and Lei, T. (2008). Investigations on fast multipole BEM in solid mechanics. *J. Univ. Sci. Technol. China*, 38(1):1–17.
138. Yotov, I. (2002). Advanced techniques and algorithms for reservoir simulation IV. Multiblock solvers and preconditioners. In Chadam, J., Cunningham, A., Ewing, R. E., and Ortoleva, P. Wheeler, M. F., editors, *IMA Volumes in Mathematics and its Applications, Volume 131: Resource Recovery, Confinement, and Remediation of Environmental Hazards*. Springer.